

# Fast two-pulse collisions in linear diffusion-advection systems with weak quadratic loss in spatial dimension 2

Avner Peleg<sup>1</sup> and Toan T. Huynh<sup>2</sup>

<sup>1</sup> *Department of Mathematics, Azrieli College of Engineering, Jerusalem 9371207, Israel and*

<sup>2</sup> *Department of Mathematics, University of Medicine and Pharmacy at Ho Chi Minh City, Ho Chi Minh City, Vietnam*

## Abstract

We investigate the dynamics of fast two-pulse collisions in linear diffusion-advection systems with weak quadratic loss in spatial dimension 2. We introduce a two-dimensional perturbation method, which generalizes the perturbation method used for studying two-pulse collisions in spatial dimension 1. We then use the generalized perturbation method to show that a fast collision in spatial dimension 2 leads to a change in the pulse shape in the direction transverse to the advection velocity vector. Moreover, we show that in the important case of a separable initial condition, the longitudinal part in the expression for the amplitude shift has a simple universal form, while the transverse part does not. Additionally, we show that anisotropy in the initial condition leads to a complex dependence of the amplitude shift on the orientation angle between the pulses. Our perturbation theory predictions are in very good agreement with results of extensive numerical simulations with the weakly perturbed diffusion-advection model. Thus, our study significantly enhances and generalizes the results of previous works on fast collisions in diffusion-advection systems, which were limited to spatial dimension 1.

## I. INTRODUCTION

Linear evolution models have a major role in many areas of physics. A central example is provided by the linear diffusion equation [1]. Other important examples include the linear wave equation [2], the linear Schrödinger equation [3], and the linear propagation equation [4–6]. Many of the physical systems that are described by linear evolution models are also affected by weak nonlinear dissipation [1, 7], and are therefore more accurately described by perturbed linear evolution models with weak nonlinear dissipation. In diffusion-advection physical systems, which are the subject of the current paper, the nonlinear dissipation arises due to chemical reactions [1, 8]. The presence of nonlinear dissipation leads to new physical effects that do not exist in the unperturbed linear physical systems. The change in pulse concentration during collisions between pulses of the linear diffusion-advection equation is an important example for such effects [9, 10]. Since the pulses of the linear physical systems and also of their weakly perturbed counterparts are not shape preserving, simple dynamics is not expected in these collisions. Consequently, one also does not expect to be able to make simple general statements about the physical effects of these collisions.

In two previous works [9, 10], we demonstrated that the opposite is in fact true in fast two-pulse collisions [11]. More specifically, we showed that the amplitude shifts in fast two-pulse collisions in linear one-dimensional physical systems with weak nonlinear dissipation exhibit simple soliton-like universal behavior. The behavior was demonstrated for two important cases: (1) systems described by the linear diffusion-advection equation with weak quadratic loss; (2) systems described by the linear propagation equation with weak cubic loss. We first developed perturbation methods for analyzing the dynamics of fast collisions in these weakly perturbed linear physical systems in spatial dimension 1. We then used the perturbation methods to show that in both systems, the expressions for the collision-induced amplitude shifts due to the nonlinear loss have the same simple universal form as the expression for the amplitude shift in a fast collision between two solitons of the nonlinear Schrödinger equation in the presence of weak cubic loss. In addition, we found that within the leading order of the perturbation theories, the pulse shapes are not changed by the collision. The predictions of the perturbation theories for the collision-induced amplitude shifts were validated by extensive numerical simulations with the two perturbed linear evolution models for a variety of initial pulse shapes [9, 10]. In addition, in Ref. [12], we showed that the perturbation

methods of Refs. [9, 10] can also be used to calculate the amplitude shifts in fast two-pulse collisions in the presence of weak high-order nonlinear loss. The results of Refs. [9, 10] are rather surprising. More specifically, the pulses in the weakly perturbed linear systems considered in these works are not shape preserving. Therefore, the common belief is that conclusions obtained from analysis of fast soliton collisions would *not* be applicable to collisions in these perturbed linear systems [13–17]. However, in Refs. [9, 10], we showed that in fact, the opposite is true.

We point out that fast two-pulse collisions in the presence of weak nonlinear effects are very important in multisequence optical communication systems [13, 18, 19]. The rates of transmission of information in these systems are significantly enhanced by transmitting many pulse sequences through the same optical medium. The pulses in each sequence propagate with the same group velocity, but the group velocities are different for pulses from different sequences. Consequently, collisions between pulses from different sequences are very frequent, and their cumulative effect can lead to severe transmission degradation and to transmission error [13, 18]. Most multisequence optical communication systems are weakly nonlinear [13, 18], and almost all collisions in these systems are fast [9, 20, 21]. Therefore, the study of fast collisions between pulses or beams of the linear propagation equation in the presence of weak nonlinearities is very relevant to multisequence optical communication links. An important question in this area concerns the characterization of the effects of a single fast two-pulse collision by explicit formulas. Indeed, such characterization enables the evaluation of the cumulative effects of many fast collisions without the need to perform a large number of numerical simulations or experiments. Furthermore, it enables the design of methods for compensating the destructive cumulative effects of the collisions.

One can adopt the concept of multisequence optical communication links in other physical systems. In particular, the concept can be implemented in diffusion-advection physical systems by transmitting many pulse sequences of different substances (different gases) through the same gaseous medium. Similar to the optical systems, the unwanted collisional effects in the chemical communication systems (due to chemical reactions) can be reduced by designing them, such that the nonlinearities are weak and the collisions are fast. Therefore, questions concerning the characterization of the effects of a single fast two-pulse collision in the presence of weak nonlinearities are of central importance for multisequence chemical communication as well. It should be mentioned that chemical and molecular communica-

tion attracted intensive research efforts in the last decades. Examples of problems considered in this area include airborne communication between mammals [22] or between plants and bacteria [23], communication mediated by pheromones [24–26], and communications in aquatic systems [27, 28]. Furthermore, controlled experiments of chemical communication via a gaseous medium with a single chemical and with two chemicals were reported in Refs. [29, 30]. The latter studies also demonstrated that the chemical communication links can indeed be described by diffusion-advection models. Thus, the possibility for realizing multisequence chemical communication provides further motivation for our current theoretical study.

The three studies in Refs. [9, 10] and [12] were limited to spatial dimension 1, and therefore, did not consider important effects, which exist only in the high-dimensional collision problem. More specifically, it is not clear if the simple universal form of the expressions for the collision-induced amplitude shifts, which was found in Refs. [9, 10] in the one-dimensional problem, remains valid in spatial dimension higher than 1. It is also unclear if the pulse shapes remain intact in the collision in the high-dimensional problem. Furthermore, high-dimensional effects due to anisotropy were not considered in Refs. [9, 10]. Thus, all the key aspects of the fast collision problem in spatial dimension higher than 1 were not addressed in previous studies. We note that the extension of the perturbation methods to dimension higher than 1 is very challenging due to the following reasons. First, it is unclear how to extend the perturbation methods in a self-consistent way, which preserves the true small parameters in the problem. Second, it is also unclear how to simplify the perturbative calculations in a manner, which allows one to obtain explicit expressions for the collision-induced changes in the pulse shape and amplitude. This is particularly true for pulses of the linear diffusion-advection equation, since these pulses are not shape preserving.

In the current work, we treat the aforementioned key aspects of the high-dimensional fast collision problem. For this purpose, we first develop a perturbation method, which generalizes the methods that were introduced in Refs. [9, 10] for the one-dimensional problem in three important ways. First, it extends the perturbative calculation from spatial dimension 1 to spatial dimension 2, and enables further extension of the calculation to a general spatial dimension. Second, it provides a calculation of the collision-induced dynamics of the pulse shape both inside and outside of the collision interval. In this way, it enables an accurate comparison between perturbation theory predictions and numerical simulations

results for the collision-induced change in the pulse shape. In contrast, the perturbative calculation of Refs. [9, 10] was restricted to the collision interval only. Third, it enables the discovery and characterization of several major collisional effects, which exist only in the high-dimensional problem. A key component in the generalization of the perturbation methods is the application of a rotation transformation, such that in the new coordinate system, the advection velocity vector (the relative velocity vector between the colliding pulses) is on the  $x$ -axis. This important step enables one to preserve the true small parameters in the problem and to obtain explicit expressions for the collision-induced changes in the pulse shape and amplitude.

We use the generalized perturbation theory to obtain formulas for the collision-induced changes in the pulse shapes and amplitudes in spatial dimension 2. We find that for a general initial condition, the collision leads to a change in the pulse shape in the direction transverse to the advection velocity vector. We then study the important case of a separable initial condition, and show that in this case, the pulse shape in the longitudinal direction is not changed by the collision in the leading order of the perturbation theory. Moreover, we show that for a separable initial condition, the longitudinal part in the expression for the amplitude shift is universal, a property that can be useful for the design of scalable multisequence chemical communication links. Additionally, the transverse part in the expression for the amplitude shift is not universal and is proportional to the integral of the product of the pulse concentrations with respect to the transverse coordinate. We also show that anisotropy in the initial condition leads to a complex dependence of the expression for the amplitude shift on the orientation angle between the colliding pulses. We attribute this complex dependence to the nonseparable character of the initial condition in the anisotropic case.

All the predictions of our perturbation theory are in very good agreement with results of extensive numerical simulations with the weakly perturbed diffusion-advection model. Therefore, our study significantly enhances and extends the results of the previous works in Refs. [9, 10] on fast two-pulse collisions in linear diffusion-advection systems with weak quadratic loss, which were limited to spatial dimension 1. It is interesting to note that we have recently found that similar high-dimensional effects exist in fast collisions between two optical beams in a linear optical medium with weak cubic loss [31]. We point out that detailed analytic results on collisions between pulse solutions of linear or nonlinear evolution models in the presence of nonlinear dissipation in spatial dimension higher than 1

are scarce, and this is especially true for pulses that are not shape preserving. Therefore, the current work and our recent work in Ref. [31] also significantly enhance the understanding of the more general high-dimensional problem of fast two-pulse collisions in the presence of nonlinear dissipation.

The remainder of the paper is organized as follows. In Sec. II, we present the generalized perturbation method for calculating the dynamics of the pulse shape and amplitude in fast collisions between pulses of the linear diffusion-advection model in spatial dimension 2. In Sec. III, we present the predictions of our perturbation theory and the results of numerical simulations with the weakly perturbed linear diffusion-advection model for three important collision setups, which demonstrate three major collisional effects that exist only in spatial dimension higher than 1. In Sec. IV, we discuss the importance of collision-induced effects due to quadratic loss in different setups of diffusion-advection systems. Section V is reserved for our conclusions. The four Appendixes contain derivations that support the material in Secs. II and III.

## II. THE PERTURBATION THEORY FOR FAST TWO-PULSE COLLISIONS IN SPATIAL DIMENSION 2

### A. Introduction

We study the dynamics of a fast collision between pulses of two substances (two gases), denoted by 1 and 2, that move in the same gaseous medium with different velocities  $\mathbf{v}_1$  and  $\mathbf{v}_2$ , and evolve in the presence of linear diffusion and weak quadratic loss in spatial dimension 2. We assume that the two pulses are injected into the gaseous medium with these velocities. Since the gaseous medium is dilute and since the collision is fast, the velocities  $\mathbf{v}_1$  and  $\mathbf{v}_2$  remain constant during the collision. We investigate the dynamics of the collision by working in the reference frame that is moving together with pulse 1. In this reference frame, pulse 1 is at rest, and pulse 2 is moving with velocity that is given by the relative velocity vector  $\mathbf{v}_d = \mathbf{v}_2 - \mathbf{v}_1$  (the advection velocity vector). This treatment is justified, since the evolution model that describes the collision dynamics is invariant under Galilean transformations. For simplicity and without loss of generality, we assume that the advection velocity vector (the relative velocity vector) lies on the  $x$  axis. Equivalently, we can say that we apply a rotation

transformation from the original coordinate system to a new coordinate system, in which the advection velocity vector is on the  $x$  axis, and that we describe the collision dynamics in the new coordinate system. In Appendix A, we show that the value of the collision-induced amplitude shift is invariant under rotation transformations in the  $xy$  plane. As a result, the choice of the advection velocity vector along the  $x$  axis does not change the value of the amplitude shift. The dynamics of the fast collision is therefore described by the following perturbed  $(2 + 1)$ -dimensional linear diffusion-advection model:

$$\begin{aligned}\partial_t u_1 &= \partial_x^2 u_1 + \partial_y^2 u_1 - \epsilon_2 u_1^2 - 2\epsilon_2 u_2 u_1, \\ \partial_t u_2 &= \partial_x^2 u_2 + \partial_y^2 u_2 - v_{d1} \partial_x u_2 - \epsilon_2 u_2^2 - 2\epsilon_2 u_1 u_2.\end{aligned}\tag{1}$$

In Eq. (1),  $u_1$  and  $u_2$  are the concentrations of substances 1 and 2,  $t$  is time,  $x$  and  $y$  are spatial coordinates,  $v_{d1}$  is the advection velocity (the velocity difference between the two pulses), and  $\epsilon_2$  is the quadratic loss coefficient, which satisfies  $0 < \epsilon_2 \ll 1$  [32]. The term  $-v_{d1} \partial_x u_2$  in Eq. (1) is an advection term due to the velocity difference between the two pulses. The terms  $-\epsilon_2 u_j^2$  and  $-2\epsilon_2 u_k u_j$  describe intra-substance and inter-substance effects due to quadratic loss, respectively. As discussed in the following paragraph, these terms are associated with chemical reactions. Note that Eq. (1) does not include linear loss terms. However, the inclusion of these terms does not alter the form of the expressions for the collision-induced changes in pulse shapes and amplitudes. Moreover, the effects of linear loss on amplitude dynamics can be incorporated in the analysis in the same manner as was done in Refs. [9, 10] for spatial dimension 1.

The quadratic loss terms in Eq. (1) are associated with chemical reactions and can be derived from the kinetic law of mass action [8, 33–35]. More specifically, the terms  $-\epsilon_2 u_1^2$  and  $-\epsilon_2 u_2^2$  are due to the reactions  $A + A \rightarrow A_2$  and  $B + B \rightarrow B_2$ , respectively. Additionally, the terms  $-2\epsilon_2 u_k u_j$  are due to the reaction  $A + B \rightarrow AB$ . We assume that the reactions products  $AB$ ,  $A_2$ , and  $B_2$  do not react with the reactants  $A$  and  $B$ , and do not dissociate, i.e., the reactions are irreversible. We remark that in Eq. (1), we consider as an example the case where the rate coefficients for the reactions  $A + A \rightarrow A_2$  and  $B + B \rightarrow B_2$  are equal to each other, and are also equal to  $1/2$  of the rate coefficient for the reaction  $A + B \rightarrow AB$ . We emphasize, however, that results similar to the ones presented in our paper are obtained in the more general case, where the rate coefficients for the reactions do not follow these simple relations. We also point out that in general, the reaction  $A + B \rightarrow AB$  is independent

of the reactions  $A + A \rightarrow A_2$ , and  $B + B \rightarrow B_2$ . Therefore, we can also consider physical setups where only the rate of the reaction  $A + B \rightarrow AB$  is significant, while the rates of the reactions  $A + A \rightarrow A_2$  and  $B + B \rightarrow B_2$  are negligible. In these physical setups, which are considered in section III D, we can neglect the terms proportional to  $-u_j^2$  in Eq. (1).

We consider fast collisions between pulses with generic initial shapes and with tails that decay sufficiently fast, such that the initial values of the total mass  $\int_{-\infty}^{\infty} dx \int_{-\infty}^{\infty} dy u_j(x, y, 0)$  are finite. We assume that the initial pulses can be characterized by initial amplitudes  $A_j(0)$ , initial widths along the  $x$  and  $y$  axes  $W_{j0}^{(x)}$  and  $W_{j0}^{(y)}$ , and initial positions  $(x_{j0}, y_{j0})$ . Thus, the initial concentrations can be written as:

$$u_j(x, y, 0) = A_j(0)h_j(x, y), \quad (2)$$

where  $h_j(x, y)$  depends on the parameters  $W_{j0}^{(x)}$ ,  $W_{j0}^{(y)}$ ,  $x_{j0}$ , and  $y_{j0}$ . We are also interested in the important case, where the initial concentrations of both substances are separable, i.e., where each of the functions  $u_j(x, y, 0)$  can be expressed as a product of a function of  $x$  and a function of  $y$ :

$$u_j(x, y, 0) = A_j(0)h_j^{(x)}[(x - x_{j0})/W_{j0}^{(x)}]h_j^{(y)}[(y - y_{j0})/W_{j0}^{(y)}]. \quad (3)$$

The separable initial condition (3) is important, since in this case one can further simplify the expressions for the collision-induced changes in pulse shapes and amplitudes and in this manner, gain deeper insight into the collision dynamics. In what follows, we will also consider cases where the initial concentration is separable for one substance and nonseparable for the other substance.

In the current paper, we are interested in the dynamics of complete fast collisions. The complete collision assumption means that the pulses are well-separated before and after the collision. Therefore, in these collisions, the values of the  $x$  coordinate of the pulse locations at  $t = 0$  and at the final time  $t_f$ ,  $x_{j0}$  and  $x_j(t_f)$ , satisfy  $|x_{20} - x_{10}| \gg W_{10}^{(x)} + W_{20}^{(x)}$  and  $|x_2(t_f) - x_1(t_f)| \gg W_1^{(x)}(t_f) + W_2^{(x)}(t_f)$ , where  $W_j^{(x)}(t_f)$  are the pulse widths in the  $x$  direction at  $t = t_f$ . The assumption of a fast collision means that the collision time interval  $\Delta t_c = 2(W_{10}^{(x)} + W_{20}^{(x)})/|v_{d1}|$ , which is the time interval during which the colliding pulses overlap, is much shorter than the smallest diffusion time in the problem. We note that the diffusion times for the  $j$ th pulse in the  $x$  and  $y$  directions are  $t_{Dj}^{(x)} = W_{j0}^{(x)2}$  and  $t_{Dj}^{(y)} = W_{j0}^{(y)2}$ , respectively. Therefore, the smallest diffusion time is  $t_D^{(min)} = \min \left\{ t_{D1}^{(x)}, t_{D2}^{(x)}, t_{D1}^{(y)}, t_{D2}^{(y)} \right\}$ .



Requiring that  $\Delta t_c \ll t_D^{(min)}$ , we find that the condition for a fast collision is  $2(W_{10}^{(x)} + W_{20}^{(x)}) \ll |v_{d1}| t_D^{(min)}$ .

Let us demonstrate that the condition for a fast collision can be realized in many weakly perturbed diffusion-advection systems. For simplicity, we look at the case where  $W_{10}^{(x)} = W_{10}^{(y)} = W_{20}^{(x)} = W_{20}^{(y)} = W_0$ , such that the fast collision condition takes the form  $W_0|v_{d1}|/4 \gg 1$ . Consider for instance diffusion of  $O_2$  in  $N_2$  at 293.15°K and at a pressure of 1 atm. The diffusion coefficient is  $D = 0.202 \text{ cm}^2/\text{s}$  [36]. Thus, for an initial pulse width of 4 cm and for an advection velocity value of  $V_{d1} = 5 \text{ cm/s}$ , we find that  $W_0|v_{d1}|/4 = 24.75$ . Similar results are obtained for other gas pairs. For example, the diffusion coefficient of  $CO_2$  in  $O_2$  at 293.15°K and at a pressure of 1 atm is  $D = 0.159 \text{ cm}^2/\text{s}$  [36]. Using this value we find that for an initial pulse width of 2 cm and for  $V_{d1} = 5 \text{ cm/s}$ ,  $W_0|v_{d1}|/4 = 15.72$ . Therefore, the condition for a fast collision is clearly satisfied in both cases.

## B. Calculation of the collision-induced effects for a general initial condition

### 1. Introduction

We introduce a perturbation method, which generalizes the perturbative calculation presented in Refs. [9, 10] in three important aspects. (1) It extends the calculation from spatial dimension 1 to spatial dimension 2, and enables further extension of the calculation to a general spatial dimension. (2) It provides a perturbative calculation of the collision-induced change in the pulse shape both in the collision interval and away from the collision interval, whereas the calculation in Refs. [9, 10] was limited to the collision interval only. This improvement enables an accurate comparison between perturbation theory predictions and numerical simulations results for the collision-induced change in the pulse shape. (3) It helps uncover several collision-induced effects, which exist only in spatial dimension higher than 1, and in this manner, enables deeper insight into the collision dynamics in the two-dimensional problem.

In the first step in the perturbative calculation, we look for a solution of Eq. (1) in the form:

$$u_j(x, y, t) = u_{j0}(x, y, t) + \phi_j(x, y, t), \quad (4)$$

where  $j = 1, 2$ ,  $u_{j0}$  are solutions of Eq. (1) without inter-pulse interaction, and  $\phi_j$  describe

collision-induced effects. By definition, the  $u_{j0}$  satisfy the following equations:

$$\partial_t u_{10} = \partial_x^2 u_{10} + \partial_y^2 u_{10} - \epsilon_2 u_{10}^2, \quad (5)$$

and

$$\partial_t u_{20} = \partial_x^2 u_{20} + \partial_y^2 u_{20} - v_{d1} \partial_x u_{20} - \epsilon_2 u_{20}^2. \quad (6)$$

We can expand the  $u_{j0}$  in perturbation series with respect to  $\epsilon_2$ :

$$u_{j0}(x, y, t) = A_j(t) \tilde{u}_{j0}(x, y, t) + \tilde{u}_{j0}^{(1)}(x, y, t) + \tilde{u}_{j0}^{(2)}(x, y, t) + \dots, \quad (7)$$

where  $A_j(t)$  are time-dependent amplitudes, and  $\tilde{u}_{j0}(x, y, t)$  are the solutions of the unperturbed linear diffusion-advection equation with unit amplitude. In addition,  $\tilde{u}_{j0}^{(1)}$  and  $\tilde{u}_{j0}^{(2)}$  are the  $O(\epsilon_2)$  and  $O(\epsilon_2^2)$  corrections to the latter solutions, and the ... stand for terms of order  $\epsilon_2^3$  and higher. It is important to note that the terms  $\tilde{u}_{j0}$ ,  $\tilde{u}_{j0}^{(1)}$ ,  $\tilde{u}_{j0}^{(2)}$  are associated with single-pulse evolution effects and not with collision-induced effects. In addition, we expand the  $\phi_j$  in perturbation series with respect to the two small parameters  $\epsilon_2$  and  $1/|v_{d1}|$ . In the current paper, we are interested in the first nonzero term in each of the expansions of the  $\phi_j$ . These first nonzero terms in the expansions clearly represent the leading-order collision-induced changes in the pulse shapes, and we therefore refer to them as the leading-order expressions for the  $\phi_j$ .

We substitute the ansatz (4) into Eq. (1) and use Eqs. (5) and (6) to obtain equations for the  $\phi_j$ . We concentrate on the calculation of  $\phi_1$ , as the calculation of  $\phi_2$  is similar. To obtain the leading-order expression for  $\phi_1$ , we neglect high-order terms containing products of  $\epsilon_2$  with  $\phi_1$  or  $\phi_2$ . In addition, in the calculation of the leading-order expression for  $\phi_1$ , we keep only the leading terms in the expansions (7). That is, in this calculation, we approximate the  $u_{j0}$  by:

$$u_{j0}(x, y, t) \simeq A_j(t) \tilde{u}_{j0}(x, y, t). \quad (8)$$

The substitution and subsequent approximations yield the following equation for the leading-order expression for  $\phi_1$ :

$$\partial_t \phi_1 = \partial_x^2 \phi_1 + \partial_y^2 \phi_1 - 2\epsilon_2 A_1(t) A_2(t) \tilde{u}_{20} \tilde{u}_{10}. \quad (9)$$

Note that for brevity and simplicity of notation, in Eq. (9), we denote the leading-order expression for  $\phi_1$  by  $\phi_1$ . This notation is also used in the remainder of the paper.

In solving the equation for  $\phi_1$ , we distinguish between two time intervals, the collision interval and the post-collision interval. To define these intervals, we introduce the collision time  $t_c$ , which is the time at which the  $x$  coordinates of the colliding pulses coincide, i.e.,  $x_1(t_c) = x_2(t_c)$ . The collision interval is the small time interval  $t_c - \Delta t_c/2 \leq t \leq t_c + \Delta t_c/2$  centered about  $t_c$ , in which the two pulses overlap. The post-collision interval is defined as the time interval  $t > t_c + \Delta t_c/2$ , in which the pulses no longer overlap.

## 2. Collision-induced effects in the collision interval

We first find the orders of the different terms in Eq. (9) in the collision interval. Since  $\Delta t_c$  is of order  $1/|v_{d1}|$ , the term  $\partial_t \phi_1$  is of order  $|v_{d1}| \times O(\phi_1)$ . The term  $-2\epsilon_2 A_1(t) A_2(t) \tilde{u}_{20} \tilde{u}_{10}$  is of order  $\epsilon_2$ . Equating the orders of  $\partial_t \phi_1$  and  $-2\epsilon_2 A_1(t) A_2(t) \tilde{u}_{20} \tilde{u}_{10}$ , we find that  $\phi_1$  is of order  $\epsilon_2/|v_{d1}|$ . In addition,  $\phi_1$  does not contain any fast dependence on  $x$  and  $y$ . Therefore, the terms  $\partial_x^2 \phi_1$  and  $\partial_y^2 \phi_1$  are of order  $\epsilon_2/|v_{d1}|$  and can be neglected. It follows that the equation for the leading-order expression for  $\phi_1$  in the collision interval is

$$\partial_t \phi_1 = -2\epsilon_2 A_1(t) A_2(t) \tilde{u}_{20} \tilde{u}_{10}. \quad (10)$$

Equation (10) has the same form as the equation obtained for a fast collision between two pulses of the linear diffusion-advection equation in the presence of weak quadratic loss in spatial dimension 1 [9, 10]. It is also similar to the equation obtained for a fast collision between two solitons of the cubic nonlinear Schrödinger equation in the presence of weak cubic loss in spatial dimension 1 [37].

A similar calculation shows that  $\phi_2$  is of order  $\epsilon_2/|v_{d1}|$ . Therefore, using Eqs. (4) and (7), we obtain that the expansions of the total concentrations  $u_j(x, y, t)$  up to second-order in the two small parameters  $\epsilon_2$  and  $1/|v_{d1}|$  are:

$$u_j(x, y, t) \simeq A_j(t) \tilde{u}_{j0}(x, y, t) + \tilde{u}_{j0}^{(1)}(x, y, t) + \tilde{u}_{j0}^{(2)}(x, y, t) + \phi_j(x, y, t). \quad (11)$$

In addition, the dynamics of the  $A_j(t)$  that is associated with single-pulse evolution is described in Appendix B.

We calculate the collision-induced amplitude shift of pulse 1 from the collision-induced change in the concentration of pulse 1,  $\Delta \phi_1(x, y, t_c) = \phi_1(x, y, t_c + \Delta t_c/2) - \phi_1(x, y, t_c - \Delta t_c/2)$ .  $\Delta \phi_1(x, y, t_c)$  is calculated by integrating Eq. (10) with respect to time over the

collision interval. This calculation yields:

$$\Delta\phi_1(x, y, t_c) = -2\epsilon_2 \int_{t_c - \Delta t_c/2}^{t_c + \Delta t_c/2} dt' A_1(t') A_2(t') \tilde{u}_{10}(x, y, t') \tilde{u}_{20}(x, y, t'). \quad (12)$$

$\tilde{u}_{20}$  is the only function in the integrand in Eq. (12) that contains fast variations in  $t$ , which are of order 1. Therefore, we can approximate  $A_1(t)$ ,  $A_2(t)$ , and  $\tilde{u}_{10}(x, y, t)$  by  $A_1(t_c^-)$ ,  $A_2(t_c^-)$ , and  $\tilde{u}_{10}(x, y, t_c)$ , where  $A_j(t_c^-)$  is the limit from the left of  $A_j$  at  $t_c$ . Furthermore, in the calculation of the integral, we can take into account in an exact manner only the fast dependence of  $\tilde{u}_{20}$  on  $t$ , i.e., the dependence on  $t$  that is contained in the factors  $\tilde{x} = x - x_{20} - v_{d1}t$ , and replace  $t$  by  $t_c$  everywhere else in the expression for  $\tilde{u}_{20}$ . We denote this approximation of  $\tilde{u}_{20}(x, y, t)$  by  $\bar{u}_{20}(\tilde{x}, y, t_c)$ . Carrying out all these approximations in Eq. (12), we obtain:

$$\begin{aligned} \Delta\phi_1(x, y, t_c) &= -2\epsilon_2 A_1(t_c^-) A_2(t_c^-) \tilde{u}_{10}(x, y, t_c) \\ &\times \int_{t_c - \Delta t_c/2}^{t_c + \Delta t_c/2} dt' \bar{u}_{20}(x - x_{20} - v_{d1}t', y, t_c). \end{aligned} \quad (13)$$

We assume that the integrand on the right hand side of Eq. (13) is sharply peaked in a small interval around  $t_c$ . As a result, we can extend the integral limits to  $-\infty$  and  $\infty$ . We also change the integration variable from  $t'$  to  $\tilde{x} = x - x_{20} - v_{d1}t'$  and obtain:

$$\Delta\phi_1(x, y, t_c) = -\frac{2\epsilon_2 A_1(t_c^-) A_2(t_c^-)}{|v_{d1}|} \tilde{u}_{10}(x, y, t_c) \int_{-\infty}^{\infty} d\tilde{x} \bar{u}_{20}(\tilde{x}, y, t_c). \quad (14)$$

We observe that the  $y$  dependence of  $\Delta\phi_1(x, y, t_c)$  is affected by the  $y$  dependence of pulse 2 at  $t = t_c$ , whereas the  $x$  dependence of  $\Delta\phi_1(x, y, t_c)$  is not affected by the  $x$  dependence of pulse 2. Therefore, inside the collision interval, the pulse shape in the longitudinal direction is retained, while the pulse shape in the transverse direction is changed. The latter collision-induced change is an effect that exists only in spatial dimension higher than 1.

One can show that the relation between the collision-induced amplitude shift of pulse 1,  $\Delta A_1^{(c)}$ , and  $\Delta\phi_1(x, y, t_c)$  is:

$$\Delta A_1^{(c)} = C_{d1}^{-1} \int_{-\infty}^{\infty} dx \int_{-\infty}^{\infty} dy \Delta\phi_1(x, y, t_c), \quad (15)$$

where

$$C_{d1} = \int_{-\infty}^{\infty} dx \int_{-\infty}^{\infty} dy \tilde{u}_{10}(x, y, 0). \quad (16)$$

Substitution of Eq. (14) into Eq. (15) yields the following expression for  $\Delta A_1^{(c)}$  for the general initial condition (2):

$$\Delta A_1^{(c)} = -\frac{2\epsilon_2 A_1(t_c^-) A_2(t_c^-)}{C_{d1} |v_{d1}|} \int_{-\infty}^{\infty} dx \int_{-\infty}^{\infty} dy \tilde{u}_{10}(x, y, t_c) \int_{-\infty}^{\infty} d\tilde{x} \bar{u}_{20}(\tilde{x}, y, t_c). \quad (17)$$

### 3. Evolution of $\phi_1(x, y, t)$ in the post-collision interval

In the post-collision interval,  $t > t_c + \Delta t_c/2$ , the colliding pulses are no longer overlapping. As a result, in this interval, the term  $-2\epsilon_2 A_1(t) A_2(t) \tilde{u}_{20} \tilde{u}_{10}$  in Eq. (9) can be neglected. Therefore, in the leading order of the calculation of the collisional effects, the equation describing the dynamics of  $\phi_1(x, y, t)$  in the post-collision interval is the unperturbed linear diffusion equation

$$\partial_t \phi_1 = \partial_x^2 \phi_1 + \partial_y^2 \phi_1. \quad (18)$$

Note that for  $|v_{d1}| \gg 1$ ,  $\Delta \phi_1(x, y, t_c) \simeq \phi_1(x, y, t_c^+)$ , where  $\phi_1(x, y, t_c^+)$  is the limit from the right of  $\phi_1(x, y, t)$  at  $t = t_c$ . Therefore, the initial condition for Eq. (18) is:

$$\phi_1(x, y, t_c^+) = \Delta \phi_1(x, y, t_c), \quad (19)$$

where  $\Delta \phi_1(x, y, t_c)$  is given by Eq. (14). The solution of Eq. (18) with the initial condition (19) is

$$\phi_1(x, y, t) = \mathcal{F}^{-1} \left( \hat{\phi}_1(k_1, k_2, t_c^+) \exp[-(k_1^2 + k_2^2)(t - t_c)] \right), \quad (20)$$

where  $\hat{\phi}_1(k_1, k_2, t_c^+) = \mathcal{F}(\phi_1(x, y, t_c^+))$ , and  $\mathcal{F}$  and  $\mathcal{F}^{-1}$  are the Fourier transform and the inverse Fourier transform with respect to  $x$  and  $y$ .

## C. Calculation of the collision-induced effects for a separable initial condition

### 1. Introduction

Let us describe the collision dynamics in the important case, where the initial condition is given by Eq. (3), i.e., it is separable for both pulses. This case is of special interest, since it is possible to further simplify the expressions for the collision-induced changes of the pulse shape and amplitude, and in this way, obtain deeper insight into the collision dynamics.

The solutions of the unperturbed linear diffusion equation with the separable initial condition (3) and with unit amplitude can be expressed in the product form:

$$\tilde{u}_{j0}(x, y, t) = g_j^{(x)}(x, t) g_j^{(y)}(y, t), \quad (21)$$

where

$$g_1^{(x)}(x, t) = (2\pi)^{-1/2} \int_{-\infty}^{\infty} dk_1 \hat{f}_1^{(x)}(k_1) \exp[-k_1^2 t + ik_1 x], \quad (22)$$

$$g_2^{(x)}(x, t) = (2\pi)^{-1/2} \int_{-\infty}^{\infty} dk_1 \hat{f}_2^{(x)}(k_1) \exp[-iv_{d1} k_1 t - k_1^2 t + ik_1 x], \quad (23)$$

and

$$g_j^{(y)}(y, t) = (2\pi)^{-1/2} \int_{-\infty}^{\infty} dk_2 \hat{f}_j^{(y)}(k_2) \exp[-k_2^2 t + ik_2 y]. \quad (24)$$

The functions  $\hat{f}_j^{(x)}(k_1)$  and  $\hat{f}_j^{(y)}(k_2)$  in Eqs. (22)-(24) are the Fourier transforms of  $h_j^{(x)}[(x - x_{j0})/W_{j0}^{(x)}]$  and  $h_j^{(y)}[(y - y_{j0})/W_{j0}^{(y)}]$ , respectively. In addition, using the conservation of the total mass for the unperturbed linear diffusion equation along with Eqs. (3) and (21), we obtain

$$\int_{-\infty}^{\infty} dx g_j^{(x)}(x, t) = \int_{-\infty}^{\infty} dx g_j^{(x)}(x, 0) = W_{j0}^{(x)} \int_{-\infty}^{\infty} ds h_j^{(x)}(s) = W_{j0}^{(x)} c_{dj}^{(x)}, \quad (25)$$

and

$$\int_{-\infty}^{\infty} dy g_j^{(y)}(y, t) = \int_{-\infty}^{\infty} dy g_j^{(y)}(y, 0) = W_{j0}^{(y)} \int_{-\infty}^{\infty} ds h_j^{(y)}(s) = W_{j0}^{(y)} c_{dj}^{(y)}, \quad (26)$$

where  $c_{dj}^{(x)}$  and  $c_{dj}^{(y)}$  are constants.

## 2. Collision-induced effects in the collision interval

We start by calculating the collision-induced change in the pulse shape in the collision-interval for an initial condition that is separable for both pulses. Note that from the definition of  $\bar{u}_{20}(\tilde{x}, y, t_c)$  it follows that  $\bar{u}_{20}(\tilde{x}, y, t_c) = \tilde{u}_{20}(x, y, t_c)$ . Using this relation together with Eqs. (21) and (25), we obtain:

$$\int_{-\infty}^{\infty} d\tilde{x} \bar{u}_{20}(\tilde{x}, y, t_c) = c_{d2}^{(x)} W_{20}^{(x)} g_2^{(y)}(y, t_c). \quad (27)$$

Substitution of Eq. (27) into Eq. (14) yields:

$$\Delta\phi_1(x, y, t_c) = -\frac{2\epsilon_2 A_1(t_c^-) A_2(t_c^-)}{|v_{d1}|} c_{d2}^{(x)} W_{20}^{(x)} g_2^{(y)}(y, t_c) \tilde{u}_{10}(x, y, t_c). \quad (28)$$

Equation (28) is valid for an initial condition that is separable for pulse 2, but not necessarily separable for pulse 1. When the initial condition is separable for pulse 1 as well, we obtain:

$$\Delta\phi_1(x, y, t_c) = -\frac{2\epsilon_2 A_1(t_c^-) A_2(t_c^-)}{|v_{d1}|} c_{d2}^{(x)} W_{20}^{(x)} g_1^{(x)}(x, t_c) g_1^{(y)}(y, t_c) g_2^{(y)}(y, t_c). \quad (29)$$

We see that the pulse shape in the longitudinal direction does not change inside the collision interval, which is similar to the behavior observed for the general initial condition [compare Eqs. (14) and (29)]. In subsection II C 3, we show that for a separable initial condition, the pulse shape in the longitudinal direction is not changed at all by the collision (within the leading order of the perturbative calculation).

Next, we calculate the collision-induced change in the pulse amplitude for a separable initial condition. Using Eqs. (16), (3), (25), and (26), we find  $C_{d1} = c_{d1}^{(x)} c_{d1}^{(y)} W_{10}^{(x)} W_{10}^{(y)}$ . In addition, using Eqs. (21) and (27), we obtain

$$\begin{aligned} \int_{-\infty}^{\infty} dx \int_{-\infty}^{\infty} dy \tilde{u}_{10}(x, y, t_c) \int_{-\infty}^{\infty} d\tilde{x} \tilde{u}_{20}(\tilde{x}, y, t_c) = \\ c_{d1}^{(x)} c_{d2}^{(x)} W_{10}^{(x)} W_{20}^{(x)} \int_{-\infty}^{\infty} dy g_1^{(y)}(y, t_c) g_2^{(y)}(y, t_c). \end{aligned} \quad (30)$$

Substitution of Eq. (30) and the expression for  $C_{d1}$  into Eq. (17) yields the following equation for  $\Delta A_1^{(c)}$  for a separable initial condition:

$$\Delta A_1^{(c)} = -\frac{2\epsilon_2 A_1(t_c^-) A_2(t_c^-)}{|v_{d1}|} \frac{c_{d2}^{(x)} W_{20}^{(x)}}{c_{d1}^{(y)} W_{10}^{(y)}} \int_{-\infty}^{\infty} dy g_1^{(y)}(y, t_c) g_2^{(y)}(y, t_c). \quad (31)$$

We observe that the expression for  $\Delta A_1^{(c)}$  has the form

$$\Delta A_1^{(c)} = -(\text{overall factor}) \times (\text{longitudinal factor}) \times (\text{transverse factor}), \quad (32)$$

where the overall factor is  $2\epsilon_2 A_1(t_c^-) A_2(t_c^-)/|v_{d1}|$ , and the longitudinal factor is  $c_{d2}^{(x)} W_{20}^{(x)}$  [38]. Application of our perturbative calculation to dimensions higher than 2 shows that the form (32) remains valid for a general spatial dimension when the initial condition is separable in the longitudinal direction for both pulses. Equation (31) is also a generalization of the equation obtained for a fast two-pulse collision in the presence of weak quadratic loss in spatial dimension 1 [compare Eq. (31) with Eq. (32) in Ref. [10]]. We also observe that

the longitudinal part in the expression for  $\Delta A_1^{(c)}$ ,  $c_{d2}^{(x)} W_{20}^{(x)}$ , is universal in the sense that it does not depend on the details of the initial pulse shapes and on the collision time  $t_c$ . In contrast, the transverse part is not universal, since it does depend on the details of the initial pulse shapes and on  $t_c$ . Thus, the universality of the expression for the amplitude shift in the one-dimensional case, which was first demonstrated in Ref. [10], is extended to spatial dimension 2 (and to spatial dimension  $n$ ), but in a somewhat restricted manner. More specifically, in the two-dimensional (and the  $n$ -dimensional) case, only the overall and longitudinal parts of the expression for  $\Delta A_1^{(c)}$  are universal, and this is true when the initial condition is separable in the longitudinal direction for both pulses.

### 3. Evolution of $\phi_1(x, y, t)$ in the post-collision interval

It is important to analyze the dynamics of  $\phi_1(x, y, t)$  in the post-collision interval for a separable initial condition for the following reasons. First, for a separable initial condition, it is possible to prove that the pulse shape in the longitudinal direction is not changed at all by the collision and this requires analysis of  $\phi_1(x, y, t)$  in the post-collision interval. Second, the simplest and clearest demonstration of the collision-induced change in pulse shape in the transverse direction is realized when the initial condition is separable for both pulses. Third, in both experiments and simulations of fast collisions, the change in the pulse shape can only be measured accurately in the post-collision interval.

The evolution of  $\phi_1$  in the post-collision interval is described by the unperturbed linear diffusion equation (18). Using Eqs. (19) and (29), we find that the initial condition for Eq. (18) is

$$\phi_1(x, y, t_c^+) = -\tilde{a}_1(t_c^-) g_1^{(x)}(x, t_c) g_{12}^{(y)}(y, t_c), \quad (33)$$

where

$$\tilde{a}_1(t_c^-) = 2\epsilon_2 A_1(t_c^-) A_2(t_c^-) c_{d2}^{(x)} W_{20}^{(x)} / |v_{d1}|, \quad (34)$$

and

$$g_{12}^{(y)}(y, t_c) = g_1^{(y)}(y, t_c) g_2^{(y)}(y, t_c). \quad (35)$$

The Fourier transform of the initial condition (33) is

$$\hat{\phi}_1(k_1, k_2, t_c^+) = -\tilde{a}_1(t_c^-) \hat{g}_1^{(x)}(k_1, t_c) \hat{g}_{12}^{(y)}(k_2, t_c), \quad (36)$$



where  $\hat{g}_1^{(x)}$  and  $\hat{g}_{12}^{(y)}$  are the Fourier transforms of  $g_1^{(x)}$  and  $g_{12}^{(y)}$  with respect to  $x$  and  $y$ , respectively. Substitution of Eq. (36) into Eq. (20) yields:

$$\begin{aligned} \phi_1(x, y, t) = & -\tilde{a}_1(t_c^-) \mathcal{F}^{-1} \left( \hat{g}_1^{(x)}(k_1, t_c) \exp[-k_1^2(t - t_c)] \right) \\ & \times \mathcal{F}^{-1} \left( \hat{g}_{12}^{(y)}(k_2, t_c) \exp[-k_2^2(t - t_c)] \right). \end{aligned} \quad (37)$$

When the initial condition for pulse 1 is separable,  $\hat{g}_1^{(x)}(k_1, t_c) \exp[-k_1^2(t - t_c)] = \hat{g}_1^{(x)}(k_1, t)$ . Using this relation in Eq. (37), we obtain the following expression for  $\phi_1(x, y, t)$  in the post-collision interval for a separable initial condition:

$$\phi_1(x, y, t) = -\tilde{a}_1(t_c^-) g_1^{(x)}(x, t) \mathcal{F}^{-1} \left( \hat{g}_{12}^{(y)}(k_2, t_c) \exp[-k_2^2(t - t_c)] \right). \quad (38)$$

Thus, when the initial condition is separable for both pulses, the  $x$  dependences of  $\phi_1(x, y, t)$  and  $\tilde{u}_{10}(x, y, t)$  are identical for  $t > t_c$ . It follows that the pulse shape in the longitudinal direction is not changed at all by the collision. Furthermore, we see that the change in the pulse shape in the transverse direction in the post-collision interval is proportional to the inverse Fourier transform of  $\hat{g}_{12}^{(y)}(k_2, t_c) \exp[-k_2^2(t - t_c)]$ .

### III. DEMONSTRATION OF NEW COLLISION-INDUCED EFFECTS IN SPATIAL DIMENSION 2

#### A. Introduction

Let us use the perturbation method of section II together with numerical simulations with Eq. (1) to demonstrate the following three major effects and properties of the collision, which exist only in spatial dimension higher than 1. (1) The universality of the longitudinal part in the expression for the collision-induced amplitude shift, an attribute that can be useful in the design of multisequence chemical communication links. (2) The effect of anisotropy in the initial condition. (3) The collision-induced change in the pulse shape in the transverse direction. For each collisional effect, we first use our perturbation method to obtain explicit approximate formulas that demonstrate the effect. We then carry out extensive numerical simulations with Eq. (1) and compare the simulations results with the approximate predictions of the perturbation method for each of the three collisional effects. We solve Eq. (1) numerically by the split-step method with periodic boundary conditions [39].

## B. Universality of the longitudinal part in the expression for the amplitude shift

In subsection IIC, we showed that for an initial condition that is separable for both pulses, the longitudinal part in the expression for the collision-induced amplitude shift is universal in the sense that it does not depend on the details of the initial pulse shapes. In the current subsection, we demonstrate this property. For this purpose, we first obtain explicit formulas for  $\Delta A_1^{(c)}$  for two initial pulse shapes that have very different dependences on the  $x$  coordinate. We then verify the validity of the formulas for  $\Delta A_1^{(c)}$  by extensive numerical simulations with Eq. (1). These simulations are very important, since they show that the approximations used in our perturbative calculation are indeed valid for very different pulse shapes. In this way, the simulations validate the theoretical prediction for universality of the expression for the amplitude shift.

The initial  $x$  dependence for the first pulse type is Gaussian, i.e., it is rapidly decreasing with increasing value of  $|x - x_{j0}|$ . In contrast, the initial  $x$  dependence for the second pulse type is given by a Cauchy-Lorentz distribution, i.e., it decreases slowly (as a power-law) with increasing value of  $|x - x_{j0}|$ . The initial pulse profile in the transverse direction is taken as Gaussian, since this choice enables the explicit calculation of the integral with respect to  $y$  on the right hand side of Eq. (31). Therefore, the two initial conditions that we consider are:

$$\begin{aligned} u_1(x, y, 0) &= A_1(0) \exp \left[ -\frac{x^2}{2W_{10}^{(x)2}} - \frac{y^2}{2W_{10}^{(y)2}} \right], \\ u_2(x, y, 0) &= A_2(0) \exp \left[ -\frac{(x - x_{20})^2}{2W_{20}^{(x)2}} - \frac{y^2}{2W_{20}^{(y)2}} \right], \end{aligned} \quad (39)$$

for Gaussian pulses, and

$$\begin{aligned} u_1(x, y, 0) &= A_1(0) \left[ 1 + \frac{2x^4}{W_{10}^{(x)4}} \right]^{-1} \exp \left[ -\frac{y^2}{2W_{10}^{(y)2}} \right], \\ u_2(x, y, 0) &= A_2(0) \left[ 1 + \frac{2(x - x_{20})^4}{W_{20}^{(x)4}} \right]^{-1} \exp \left[ -\frac{y^2}{2W_{20}^{(y)2}} \right], \end{aligned} \quad (40)$$

for Cauchy-Lorentz-Gaussian pulses.

We first obtain the expression for the collision-induced amplitude shift for the initial conditions (39) and (40). From Eq. (C5) it follows that for both initial conditions

$$g_j^{(y)}(y, t_c) = \frac{W_{j0}^{(y)}}{(W_{j0}^{(y)2} + 2t_c)^{1/2}} \exp \left[ -\frac{y^2}{2W_{j0}^{(y)2} + 4t_c} \right]. \quad (41)$$

In addition,  $c_{d1}^{(y)} = (2\pi)^{1/2}$  in both cases. We substitute Eq. (41) and the value of  $c_{d1}^{(y)}$  into Eq. (31), and carry out the integration with respect to  $y$ . We obtain the following expression for  $\Delta A_1^{(c)}$ :

$$\Delta A_1^{(c)} = -\frac{2\epsilon_2 A_1(t_c^-) A_2(t_c^-)}{|v_{d1}|} \frac{c_{d2}^{(x)} W_{20}^{(x)} W_{20}^{(y)}}{(W_{10}^{(y)2} + W_{20}^{(y)2} + 4t_c)^{1/2}}, \quad (42)$$

where  $c_{d2}^{(x)} = (2\pi)^{1/2}$  for Gaussian pulses, and  $c_{d2}^{(x)} = \pi/2^{3/4}$  for Cauchy-Lorentz-Gaussian pulses. We observe that the longitudinal part in the expression for  $\Delta A_1^{(c)}$ ,  $c_{d2}^{(x)} W_{20}^{(x)}$ , is universal. In contrast, the transverse part, which is given by:

$$\text{transverse factor} = \frac{W_{20}^{(y)}}{(W_{10}^{(y)2} + W_{20}^{(y)2} + 4t_c)^{1/2}}, \quad (43)$$

depends on  $t_c$ , and does not possess a simple universal form like the longitudinal part. An important aspect of the nonuniversal nature of the equation for  $\Delta A_1^{(c)}$  in spatial dimension 2 is the deviation of the dependence on  $|v_{d1}|$  from the  $1/|v_{d1}|$  scaling that exists in the one-dimensional case [9, 10], and also in fast collisions between solitons of the nonlinear Schrödinger equation in the presence of weak nonlinear dissipation in spatial dimension 1 [37, 40]. Indeed, the collision time  $t_c$  is given by  $t_c = (x_{10} - x_{20})/v_{d1}$ . Therefore, the deviation of the  $|v_{d1}|$  dependence of  $\Delta A_1^{(c)}$  from the  $1/|v_{d1}|$  scaling is due to the term  $4t_c = 4(x_{10} - x_{20})/v_{d1}$  in the factor  $(W_{10}^{(y)2} + W_{20}^{(y)2} + 4(x_{10} - x_{20})/v_{d1})^{1/2}$  on the right hand side of Eq. (42). To characterize the latter deviation, we define the quantity  $\Delta A_1^{(c)(s)}$ , which is the approximate expression for the amplitude shift that is obtained from the full expression by neglecting the  $4(x_{10} - x_{20})/v_{d1}$  term. By this definition,  $\Delta A_1^{(c)(s)}$  is given by:

$$\Delta A_1^{(c)(s)} = -\frac{2\epsilon_2 A_1(t_c^-) A_2(t_c^-)}{|v_{d1}|} \frac{c_{d2}^{(x)} W_{20}^{(x)} W_{20}^{(y)}}{(W_{10}^{(y)2} + W_{20}^{(y)2})^{1/2}}. \quad (44)$$

Thus, the difference  $|\Delta A_1^{(c)} - \Delta A_1^{(c)(s)}|$  is a measure for the departure of the  $|v_{d1}|$  dependence of  $\Delta A_1^{(c)}$  from the  $1/|v_{d1}|$  scaling observed in the one-dimensional case. Since in a complete collision  $|x_{20} - x_{10}| \gg 1$ , the term  $4(x_{10} - x_{20})/v_{d1}$  is not necessarily small for intermediate values of  $|v_{d1}|$ . As a result, the departure from the  $1/|v_{d1}|$  scaling might be substantial even for intermediate  $|v_{d1}|$  values.

We check the perturbation theory predictions for universality of the longitudinal part in the expression for  $\Delta A_1^{(c)}$  by performing numerical simulations with Eq. (1) with the two initial conditions (39) and (40). The extensive simulations with these initial conditions

provide a careful test for the validity of the perturbation theory approximations for widely different pulse shapes. In this manner, the simulations help validate the universality of the longitudinal part in the expression for  $\Delta A_1^{(c)}$ . We are interested in fast collisions in the presence of weak quadratic loss. Therefore, we carry out the simulations with  $\epsilon_2 = 0.01$  and with  $v_{d1}$  values in the intervals  $4 \leq |v_{d1}| \leq 60$ . The parameter values of the initial conditions (39) and (40) are  $A_j(0) = 1$ ,  $x_{20} = \pm 20$ ,  $W_{10}^{(x)} = 3$ ,  $W_{10}^{(y)} = 5$ ,  $W_{20}^{(x)} = 4$ , and  $W_{20}^{(y)} = 6$ . The final time is  $t_f = 2t_c = -2x_{20}/v_{d1}$ . The values of  $x_{20}$  and  $t_f$  ensure that the colliding pulses are well separated at  $t = 0$  and at  $t = t_f$ . We emphasize that results similar to the ones described here are obtained in simulations with other parameter values. For each initial condition, we compare the dependence of  $\Delta A_1^{(c)}$  on  $v_{d1}$  obtained in the simulations with the perturbation theory prediction of Eq. (42), and with the crude approximation of Eq. (44). We also discuss the behavior of the relative errors in the approximation of the amplitude shift (in percentage), which are defined by  $E_r^{(1)} = |\Delta A_1^{(c)(num)} - \Delta A_1^{(c)(th)}| \times 100/|\Delta A_1^{(c)(th)}|$  and  $E_r^{(2)} = |\Delta A_1^{(c)(num)} - \Delta A_1^{(c)(s)}| \times 100/|\Delta A_1^{(c)(s)}|$ , respectively.

We first discuss the results of the simulations for fast collisions between pulses with rapidly decaying tails, which are represented by Gaussian pulses. The initial pulse shapes  $u_j(x, y, 0)$ , and the pulse shapes  $u_j(x, y, t)$  obtained in the simulation with  $v_{d1} = 10$  at the intermediate time  $t_i = 2.4 > t_c$  [41], and at the final time  $t_f = 4$  are shown in Fig. 1. We observe that the pulses experience broadening due to diffusion. We also observe that the maximum values of  $u_j(x, y, t)$  decrease with increasing time, mainly due to diffusion. The dependence of  $\Delta A_1^{(c)}$  on  $v_{d1}$  obtained in the simulations is shown in Fig. 2 together with the analytic predictions  $\Delta A_1^{(c)}$  and  $\Delta A_1^{(c)(s)}$  of Eqs. (42) and (44). The agreement between the simulations result and the analytic prediction of Eq. (42) is very good despite the diffusion-induced pulse broadening. More specifically, the relative error  $E_r^{(1)}$  is smaller than 2.4% for  $10 \leq |v_{d1}| \leq 60$  and smaller than 5.4% for  $4 \leq |v_{d1}| < 10$ . We also note that the relative error  $E_r^{(2)}$  is smaller than 8.2% for  $10 \leq |v_{d1}| \leq 60$  and smaller than 17.9% for  $4 \leq |v_{d1}| < 10$ . The latter values are noticeably larger than the corresponding values of  $E_r^{(1)}$ . Thus, in accordance with the perturbation theory prediction, the deviation of the  $v_{d1}$  dependence of  $\Delta A_1^{(c)}$  from the  $1/|v_{d1}|$  scaling is noticeable already at intermediate  $|v_{d1}|$  values, and it increases with decreasing values of  $|v_{d1}|$ .

Let us discuss the simulations results for fast collisions between pulses with slowly decaying tails in the longitudinal direction, which are represented by Cauchy-Lorentz-Gaussian

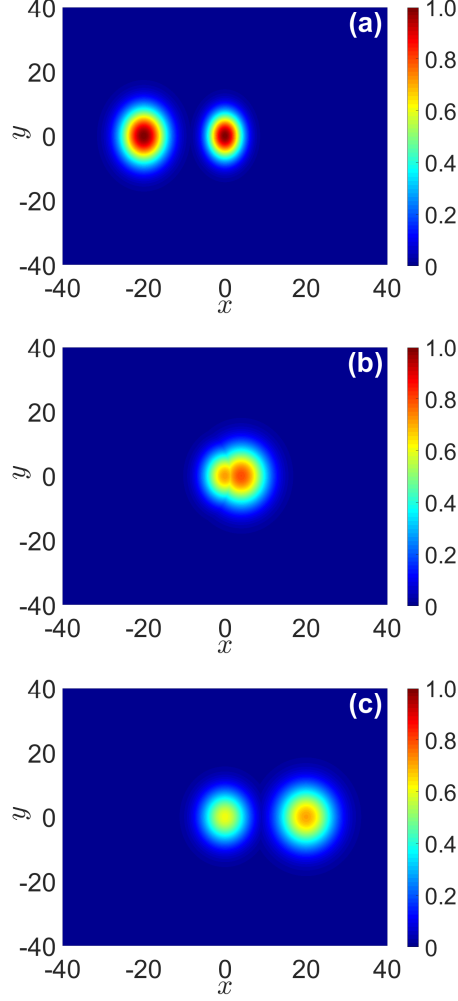


FIG. 1: (Color online) Contour plots of the pulse shapes  $u_j(x, y, t)$  at  $t = 0$  (a),  $t = t_i = 2.4$  (b), and  $t = t_f = 4$  (c) in a fast collision between two Gaussian pulses with parameter values  $\epsilon_2 = 0.01$  and  $v_{d1} = 10$ . The plots represent the pulse shapes obtained by numerical solution of Eq. (1) with the initial condition (39).

pulses. In this case, it is unclear if the sharp-peak approximation that is used in the derivation of Eq. (14) is valid. Therefore, the simulations of fast collisions between Cauchy-Lorentz-Gaussian pulses serve as an important check of both the perturbation theory approximations and the perturbation theory prediction for universality of the longitudinal part in the expression for  $\Delta A_1^{(c)}$ . Figure 3 shows the pulse shapes  $u_j(x, y, t)$  obtained in the simulation with  $v_{d1} = 10$  at  $t = 0$ ,  $t_i = 2.4$ , and  $t_f = 4$ . It is seen that the pulses undergo significant broadening due to diffusion, and that the maximum values of  $u_j(x, y, t)$  decrease with increasing  $t$  as a result. The numerically obtained dependence of  $\Delta A_1^{(c)}$  on  $v_{d1}$  is shown

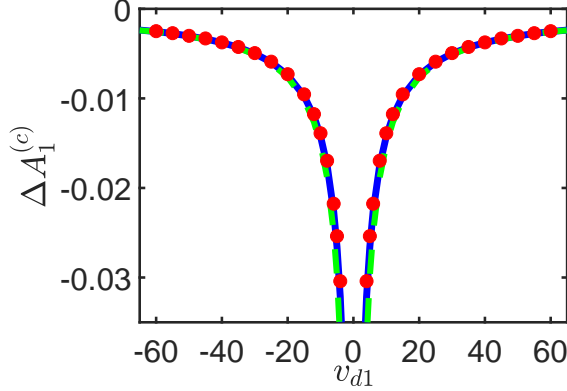


FIG. 2: (Color online) The collision-induced amplitude shift of pulse 1  $\Delta A_1^{(c)}$  vs advection velocity  $v_{d1}$  in a fast collision between two Gaussian pulses for  $\epsilon_2 = 0.01$ . The red circles represent the result obtained by numerical simulations with Eq. (1) with the initial condition (39). The solid blue and dashed green curves correspond to the theoretical predictions of Eqs. (42) and (44), respectively.

in Fig. 4 along with the perturbation theory predictions of Eqs. (42) and (44). We observe very good agreement between the simulations result and the analytic prediction of Eq. (42) despite the significant pulse broadening. In particular, the relative error  $E_r^{(1)}$  is smaller than 2.1% for  $10 \leq |v_{d1}| \leq 60$  and smaller than 4.5% for  $4 \leq |v_{d1}| < 10$ . These values are comparable to the values of  $E_r^{(1)}$  for collisions between Gaussian pulses. Thus, based on the results shown in Figs. 2 and 4 and on similar results obtained with other values of the physical parameters, we conclude that the longitudinal part in the expression for  $\Delta A_1^{(c)}$  is indeed universal in the sense that it is not very sensitive to the details of the initial pulse shapes. We also note that the values of  $E_r^{(2)}$  obtained in collisions between Cauchy-Lorentz-Gaussian pulses are noticeably larger than the corresponding values of  $E_r^{(1)}$  for intermediate and small  $|v_{d1}|$  values. Therefore, our simulations also demonstrate that the departure of the  $v_{d1}$  dependence of  $\Delta A_1^{(c)}$  from the  $1/|v_{d1}|$  scaling is noticeable already at intermediate values of  $|v_{d1}|$ .

### C. Dependence of the amplitude shift on the inter-pulse orientation angle

Another phenomenon that exists only in spatial dimension higher than 1 is associated with the effects of anisotropy in the physical system. In the current paper, we are interested in studying the effects of anisotropy in the initial condition. In a simple setup, this anisotropy

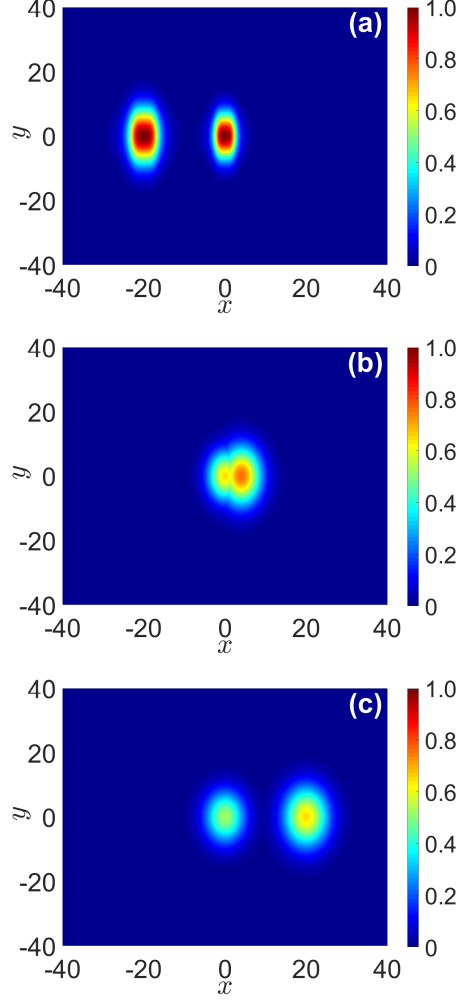


FIG. 3: (Color online) Contour plots of the pulse shapes  $u_j(x, y, t)$  at  $t = 0$  (a),  $t = t_i = 2.4$  (b), and  $t = t_f = 4$  (c) in a fast collision between two Cauchy-Lorentz-Gaussian pulses with parameter values  $\epsilon_2 = 0.01$  and  $v_{d1} = 10$ . The plots represent the pulse shapes obtained by numerical solution of Eq. (1) with the initial condition (40).

can be characterized by a single angle  $\theta_0$ , e.g., the angle between a “preferred” direction in the initial condition and the  $x$  axis. Consider as an example the case where the initial width of pulse 1 along one direction, which we denote by  $x'$ , is larger than the initial width along the perpendicular direction  $y'$ . We then define  $\theta_0$  as the angle that the  $x'$  axis forms with the  $x$  axis of our coordinate system. Therefore,  $\theta_0$  is the angle between the advection velocity vector and the  $x'$  axis. In addition, if pulse 2 is circularly symmetric, or is elongated along the  $x$  or the  $y$  axes, then  $\theta_0$  can also be regarded as the orientation angle between the two pulses. A central question about the collision dynamics in this setup concerns the dependence of

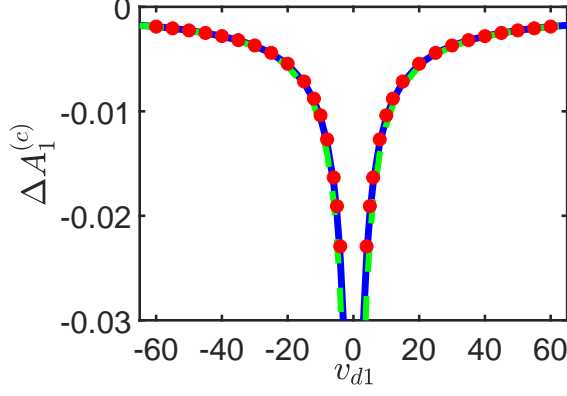


FIG. 4: (Color online) The collision-induced amplitude shift of pulse 1  $\Delta A_1^{(c)}$  vs advection velocity  $v_{d1}$  in a fast collision between two Cauchy-Lorentz-Gaussian pulses for  $\epsilon_2 = 0.01$ . The red circles represent the result obtained by numerical simulations with Eq. (1) with the initial condition (40). The solid blue and dashed green curves represent the theoretical predictions of Eqs. (42) and (44), respectively.

the amplitude shift  $\Delta A_1^{(c)}$  on the orientation angle  $\theta_0$ . In the current subsection, we address this central question both analytically and by numerical simulations.

We consider an anisotropic collision setup, consisting of two initially well separated Gaussian pulses. In addition, pulse 1 is elongated along its  $x'$  axis, which forms an angle  $\theta_0$  with the  $x$  axis, while pulse 2 is circularly symmetric. Figure 5(a) shows the contour plot of  $u_j(x, y, 0)$  for this anisotropic initial condition in the case  $\theta_0 = \pi/4$ . The initial condition can be expressed as:

$$u'_1(x', y', 0) = A_1(0) \exp \left[ -\frac{x'^2}{2W_{10}^{(x)2}} - \frac{y'^2}{2W_{10}^{(y)2}} \right], \quad (45)$$

and

$$u_2(x, y, 0) = A_2(0) \exp \left[ -\frac{(x - x_{20})^2}{2W_{20}^2} - \frac{y^2}{2W_{20}^2} \right], \quad (46)$$

where  $u'_1(x', y', t)$  is the concentration of pulse 1 in the  $(x', y', t)$  coordinate system,  $W_{10}^{(x)} > W_{10}^{(y)}$ , and

$$\begin{aligned} x' &= x \cos \theta_0 + y \sin \theta_0, \\ y' &= -x \sin \theta_0 + y \cos \theta_0. \end{aligned} \quad (47)$$



Substituting Eq. (47) into Eq. (45), we obtain:

$$u_1(x, y, 0) = A_1(0) \exp [-B_1 x^2 - B_2 y^2 - B_3 xy], \quad (48)$$

where

$$B_1 = \frac{\cos^2 \theta_0}{2W_{10}^{(x)2}} + \frac{\sin^2 \theta_0}{2W_{10}^{(y)2}},$$

$$B_2 = \frac{\sin^2 \theta_0}{2W_{10}^{(x)2}} + \frac{\cos^2 \theta_0}{2W_{10}^{(y)2}},$$

and

$$B_3 = \left( \frac{1}{W_{10}^{(x)2}} - \frac{1}{W_{10}^{(y)2}} \right) \sin \theta_0 \cos \theta_0.$$

Note that the initial condition for pulse 1 in the  $(x, y, t)$  coordinate system is not separable, and therefore the current investigation also provides an example for collision-induced dynamics with a nonseparable initial condition.

Since the initial condition for pulse 1 is nonseparable, we calculate  $\Delta A_1^{(c)}$  by using the general expression of Eq. (17). For the current setup,  $C_{d1} = 2\pi W_{10}^{(x)} W_{10}^{(y)}$ . Additionally, the initial condition for pulse 2 is separable, and as a result, we can use Eq. (27), where  $c_{d2}^{(x)} = (2\pi)^{1/2}$ . Substituting these relations into Eq. (17), we obtain

$$\Delta A_1^{(c)} = -\frac{2^{1/2} \epsilon_2 A_1(t_c^-) A_2(t_c^-)}{\pi^{1/2} |v_{d1}|} \frac{W_{20}}{W_{10}^{(x)} W_{10}^{(y)}} \int_{-\infty}^{\infty} dy g_2^{(y)}(y, t_c) \int_{-\infty}^{\infty} dx \tilde{u}_{10}(x, y, t_c). \quad (49)$$

Since diffusion is isotropic, the unperturbed diffusion equation for pulse 1 in the  $(x', y', t)$  coordinate system is:

$$\partial_t \tilde{u}'_{10} = \partial_{x'}^2 \tilde{u}'_{10} + \partial_{y'}^2 \tilde{u}'_{10}. \quad (50)$$

Therefore, we can calculate  $\tilde{u}_{10}(x, y, t)$  by solving Eq. (50) with the initial condition (45) in the  $(x', y', t)$  coordinate system, and by expressing the solution in the  $(x, y, t)$  coordinate system with the help of Eq. (47). Carrying out this calculation and multiplying the result by  $g_2^{(y)}(y, t_c)$ , we obtain:

$$g_2^{(y)}(y, t_c) \tilde{u}_{10}(x, y, t_c) = \frac{W_{10}^{(x)} W_{10}^{(y)} W_{20}}{(W_{10}^{(x)2} + 2t_c)^{1/2} (W_{10}^{(y)2} + 2t_c)^{1/2} (W_{20}^2 + 2t_c)^{1/2}} \times \exp [-b_1^2 x^2 - 2b_2 xy - b_3^2 y^2], \quad (51)$$

where

$$b_1 = \left( \frac{\cos^2 \theta_0}{2W_{10}^{(x)2} + 4t_c} + \frac{\sin^2 \theta_0}{2W_{10}^{(y)2} + 4t_c} \right)^{1/2}, \quad (52)$$

$$b_2 = \left( \frac{1}{2W_{10}^{(x)2} + 4t_c} - \frac{1}{2W_{10}^{(y)2} + 4t_c} \right) \sin \theta_0 \cos \theta_0, \quad (53)$$

$$b_3 = \left( \frac{1}{2W_{20}^2 + 4t_c} + \frac{\sin^2 \theta_0}{2W_{10}^{(x)2} + 4t_c} + \frac{\cos^2 \theta_0}{2W_{10}^{(y)2} + 4t_c} \right)^{1/2}. \quad (54)$$

Substitution of Eq. (51) into Eq. (49) and integration with respect to  $x$  and  $y$  yield the following expression for  $\Delta A_1^{(c)}$ :

$$\begin{aligned} \Delta A_1^{(c)} &= \frac{-(2\pi)^{1/2} \epsilon_2 A_1(t_c^-) A_2(t_c^-)}{|v_{d1}|} \\ &\times \frac{W_{20}^2}{\left(W_{10}^{(x)2} + 2t_c\right)^{1/2} \left(W_{10}^{(y)2} + 2t_c\right)^{1/2} (W_{20}^2 + 2t_c)^{1/2} (b_1^2 b_3^2 - b_2^2)^{1/2}}, \end{aligned} \quad (55)$$

where

$$\begin{aligned} b_1^2 b_3^2 - b_2^2 &= \frac{1}{2W_{20}^2 + 4t_c} \left( \frac{\cos^2 \theta_0}{2W_{10}^{(x)2} + 4t_c} + \frac{\sin^2 \theta_0}{2W_{10}^{(y)2} + 4t_c} \right) \\ &+ \frac{1}{\left(2W_{10}^{(x)2} + 4t_c\right) \left(2W_{10}^{(y)2} + 4t_c\right)}. \end{aligned} \quad (56)$$

Thus, even in the simple anisotropic collision setup considered here, the dependence of  $\Delta A_1^{(c)}$  on the orientation angle  $\theta_0$  is complex. This complex dependence of  $\Delta A_1^{(c)}$  on  $\theta_0$  can also be related to the nonseparable nature of the initial condition for pulse 1.

We check the perturbation theory prediction of Eq. (55) for the dependence of  $\Delta A_1^{(c)}$  on the orientation angle  $\theta_0$  by numerical simulations with Eq. (1) with the initial condition of Eqs. (46) and (48). The simulations are carried out for  $\theta_0$  values in the interval  $0 \leq \theta_0 \leq \pi/2$ , and with physical parameter values  $\epsilon_2 = 0.01$  and  $v_{d1} = 20$ . The initial pulse parameters values are  $A_j(0) = 1$ ,  $x_{20} = -20$ ,  $W_{10}^{(x)} = 8$ ,  $W_{10}^{(y)} = 2$ , and  $W_{20} = 2$ . The final time is  $t_f = 2$ , and therefore, the pulses are well separated at  $t_f$ . The initial pulse shapes  $u_j(x, y, 0)$ , and the pulse shapes  $u_j(x, y, t)$  obtained in the simulation with  $\theta_0 = \pi/4$  at the intermediate time  $t_i = 1.2 > t_c$ , and at  $t_f = 2$  are shown in Fig. 5. We observe that both pulses undergo

significant broadening due to diffusion, and that the maximum values of  $u_j(x, y, t)$  decrease with increasing time. The dependence of  $\Delta A_1^{(c)}$  on  $\theta_0$  obtained in the simulations is shown in Fig. 6 along with the theoretical prediction of Eq. (55). The agreement between the simulations result and the perturbation theory prediction is very good. More specifically, the relative error (in percentage)  $|\Delta A_1^{(c)(num)} - \Delta A_1^{(c)(th)}| \times 100 / |\Delta A_1^{(c)(th)}|$  is smaller than 2.9% in the entire interval  $0 \leq \theta_0 \leq \pi/2$ . Therefore, the numerical simulations validate the perturbation theory prediction for a complex dependence of  $\Delta A_1^{(c)}$  on  $\theta_0$  due to the anisotropic (and nonseparable) character of the initial condition.

#### D. Collision-induced change in the pulse shape

The collision-induced change in the pulse shape in the transverse direction, which was uncovered by our perturbation theory in subsection II B, is an important collisional effect that exists only in spatial dimension higher than 1. Indeed, it was shown in Refs. [9, 10] that within the leading order of the perturbative calculation, the pulse shape is preserved during a fast two-pulse collision in the presence of weak quadratic loss in spatial dimension 1. In the current subsection, we investigate this important high-dimensional effect of the collision in detail both analytically and by numerical simulations.

To enable a more accurate comparison between the perturbative calculation and the numerical simulations, we assume that the effects of quadratic loss on single-pulse evolution, which are described by the terms proportional to  $-u_j^2$  in Eq. (1), are negligible. This assumption is valid when the rates of the reactions  $A + A \rightarrow A_2$  and  $B + B \rightarrow B_2$  are much smaller than the rate of the reaction  $A + B \rightarrow AB$ . Furthermore, from Eq. (8) it follows that the terms  $\tilde{u}_{j0}^{(1)}$ ,  $\tilde{u}_{j0}^{(2)}$ , etc. in the expansions (7) of the  $u_{j0}$  do not contribute to the leading-order expression for the collision-induced change in the pulse shape  $\phi_1$ . Therefore, the omission of the  $-u_j^2$  terms in Eq. (1) is also mathematically consistent, since it does not affect the perturbation theory prediction and the numerical simulation result for the leading-order expression for  $\phi_1$ . Neglecting the terms proportional to  $-u_j^2$  in Eq. (1), we obtain the following perturbed linear diffusion-advection equation for the collision dynamics:

$$\begin{aligned}\partial_t u_1 &= \partial_x^2 u_1 + \partial_y^2 u_1 - 2\epsilon_2 u_2 u_1, \\ \partial_t u_2 &= \partial_x^2 u_2 + \partial_y^2 u_2 - v_{d1} \partial_x u_2 - 2\epsilon_2 u_1 u_2,\end{aligned}\tag{57}$$

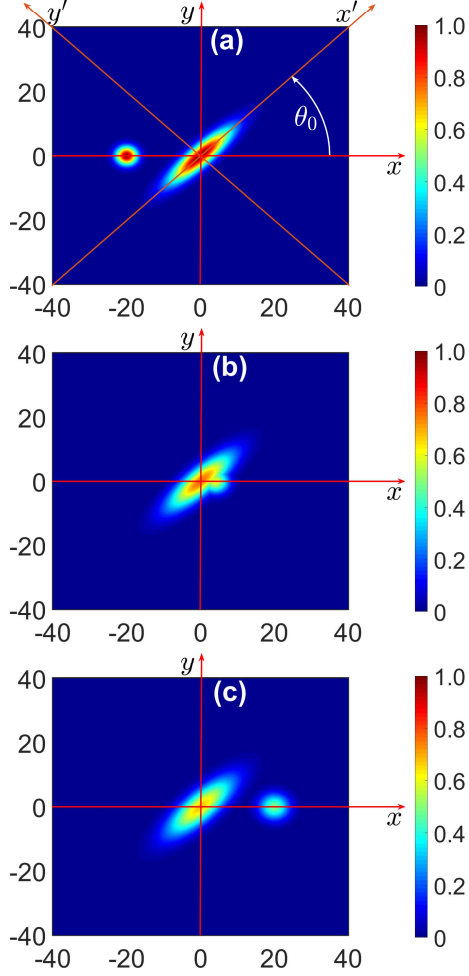


FIG. 5: (Color online) Contour plots of the pulse shapes  $u_j(x, y, t)$  at  $t = 0$  (a),  $t = t_i = 1.2$  (b), and  $t = t_f = 2$  (c) in a fast collision between two Gaussian pulses with the anisotropic initial condition of Eqs. (46) and (48). The orientation angle is  $\theta_0 = \pi/4$ . The plots in (b) and (c) represent the pulse shapes obtained by numerical solution of Eq. (1) with physical parameter values  $\epsilon_2 = 0.01$  and  $v_{d1} = 20$ .

where  $0 < \epsilon_2 \ll 1$ . We consider a collision between two Gaussian pulses as a concrete example. Therefore, the initial condition for the collision problem is given by Eq. (39). With this choice of the initial condition we can obtain an explicit formula for the collision-induced change in the shape of pulse 1  $\phi_1$  in the post-collision interval.

We note that the initial condition (39) is separable for both pulses. Therefore, we can calculate  $\phi_1$  in the post-collision interval by using Eq. (38). Additionally, since the effects of quadratic loss on single-pulse evolution are negligible, we can replace  $A_j(t_c^-)$  by  $A_j(0)$

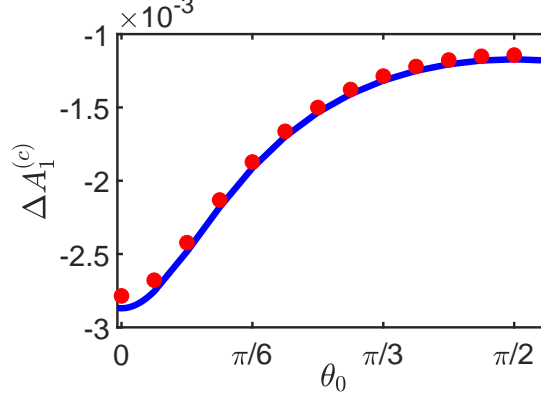


FIG. 6: (Color online) The collision-induced amplitude shift of pulse 1  $\Delta A_1^{(c)}$  vs the orientation angle  $\theta_0$  in a fast collision between two Gaussian pulses with the anisotropic initial condition of Eqs. (46) and (48). The red circles represent the result obtained by numerical simulations with Eq. (1). The solid blue curve corresponds to the perturbation theory prediction of Eq. (55).

everywhere in the calculation. Therefore, the coefficient  $\tilde{a}_1$  of Eq. (34) is given by [42]:

$$\tilde{a}_1 = (8\pi)^{1/2} \epsilon_2 A_1(0) A_2(0) W_{20}^{(x)} / |v_{d1}|. \quad (58)$$

The function  $g_1^{(x)}(x, t)$  in Eq. (38) is given by Eq. (C4) in Appendix C. In addition, in Appendix D, we show that

$$\begin{aligned} \mathcal{F}^{-1} \left( \hat{g}_{12}^{(y)}(k_2, t_c) \exp[-k_2^2(t - t_c)] \right) &= \frac{W_{10}^{(y)} W_{20}^{(y)}}{(W_{10}^{(y)2} + 2t_c)^{1/2} (W_{20}^{(y)2} + 2t_c)^{1/2} [1 + 4\tilde{a}_2^2(t_c)(t - t_c)]^{1/2}} \\ &\times \exp \left[ -\frac{\tilde{a}_2^2(t_c) y^2}{1 + 4\tilde{a}_2^2(t_c)(t - t_c)} \right], \end{aligned} \quad (59)$$

where  $\tilde{a}_2^2(t_c)$  is given by Eq. (D2). Substitution of Eqs. (58), (59), and (C4) into Eq. (38) yields the following expression for  $\phi_1(x, y, t)$  in the post-collision interval:

$$\begin{aligned} \phi_1(x, y, t) &= -\frac{\tilde{a}_1 W_{10}^{(x)} W_{10}^{(y)} W_{20}^{(y)}}{(W_{10}^{(x)2} + 2t)^{1/2} (W_{10}^{(y)2} + 2t_c)^{1/2} (W_{20}^{(y)2} + 2t_c)^{1/2} [1 + 4\tilde{a}_2^2(t_c)(t - t_c)]^{1/2}} \\ &\times \exp \left[ -\frac{x^2}{2W_{10}^{(x)2} + 4t} - \frac{\tilde{a}_2^2(t_c) y^2}{1 + 4\tilde{a}_2^2(t_c)(t - t_c)} \right]. \end{aligned} \quad (60)$$

Further insight into the collision-induced change in the pulse shape can be gained by analyzing the fractional concentration reduction factor  $\Delta\phi_1^{(r)}$ . In the current collision setup, the effects of quadratic loss on single-pulse evolution are negligible. As a result, in this case,

$u_{j0}(x, y, t) = A_j(0)\tilde{u}_{j0}(x, y, t)$ , and from Eq. (4) we obtain:  $u_j(x, y, t) = A_j(0)\tilde{u}_{j0}(x, y, t) + \phi_j(x, y, t)$ . Thus, in the current collision setup, we define  $\Delta\phi_1^{(r)}$  by:

$$\Delta\phi_1^{(r)}(x, y, t) = \frac{A_1(0)\tilde{u}_{10}(x, y, t) - u_1(x, y, t)}{A_1(0)\tilde{u}_{10}(x, y, t)} = -\frac{\phi_1(x, y, t)}{A_1(0)\tilde{u}_{10}(x, y, t)}. \quad (61)$$

We see that the fractional concentration reduction factor measures the ratio between the concentration decrease of pulse 1, which is induced by the effects of quadratic loss on the collision, and the concentration of pulse 1 in the unperturbed single-pulse evolution problem. Note that for a separable initial condition, the  $x$  dependences of  $\tilde{u}_{10}$  and of the leading order expression for  $\phi_1$  are identical. Therefore, in this case, the  $x$  dependence cancels out on the right hand side of Eq. (61), and  $\Delta\phi_1^{(r)}$  becomes a function of  $y$  and  $t$  only.

We check the perturbation theory predictions for the collision-induced change in the pulse shape by extensive numerical simulations with Eq. (57). We perform the simulations with  $\epsilon_2 = 0.01$  and with  $v_{d1}$  values satisfying  $4 \leq |v_{d1}| \leq 60$ . The parameter values of the initial condition (39) are  $A_j(0) = 1$ ,  $x_{20} = \pm 20$ ,  $W_{10}^{(x)} = 3$ ,  $W_{10}^{(y)} = 2$ ,  $W_{20}^{(x)} = 2$ , and  $W_{20}^{(y)} = 1$ . The final time is  $t_f = 2t_c = -2x_{20}/v_{d1}$ , and therefore, the pulses are well separated at  $t_f$ . The contour plots of the pulse shapes  $u_j(x, y, t)$  obtained in the simulations are similar to the ones seen in Fig. 1. In particular, the pulses undergo significant diffusion-induced broadening, and the maximum values of  $u_j(x, y, t)$  decrease with increasing  $t$ . The collision-induced change in the shape of pulse 1 that is obtained in the simulation with  $v_{d1} = 25$  at  $t = t_f$ ,  $\phi_1^{(num)}(x, y, t_f)$ , is shown in Fig. 7. The perturbation theory prediction,  $\phi_1^{(th)}(x, y, t_f)$ , which is obtained by Eq. (60), is also shown. The agreement between the simulation result and the perturbation theory prediction is excellent. To quantify the deviation of  $\phi_1^{(th)}(x, y, t)$  from  $\phi_1^{(num)}(x, y, t)$ , we define the relative error (in percentage)  $E_r^{(\phi_1)}(t)$  by:

$$E_r^{(\phi_1)}(t) = 100 \times \left[ \int dx \int dy |\phi_1^{(th)}(x, y, t)|^2 \right]^{-1/2} \times \left\{ \int dx \int dy \left[ \left| \phi_1^{(th)}(x, y, t) \right| - \left| \phi_1^{(num)}(x, y, t) \right| \right]^2 \right\}^{1/2}, \quad (62)$$

where the integration is performed over the entire simulation domain in the  $xy$  plane. We find that the value of  $E_r^{(\phi_1)}(t_f)$  is 0.82% for  $v_{d1} = 25$ , in accordance with the excellent agreement between simulation and theory observed in Fig. 7.

As a further check of the perturbation theory prediction, we analyze the  $y$  dependence of the fractional concentration reduction factor  $\Delta\phi_1^{(r)}$ . Figure 8 shows the  $y$  dependence of

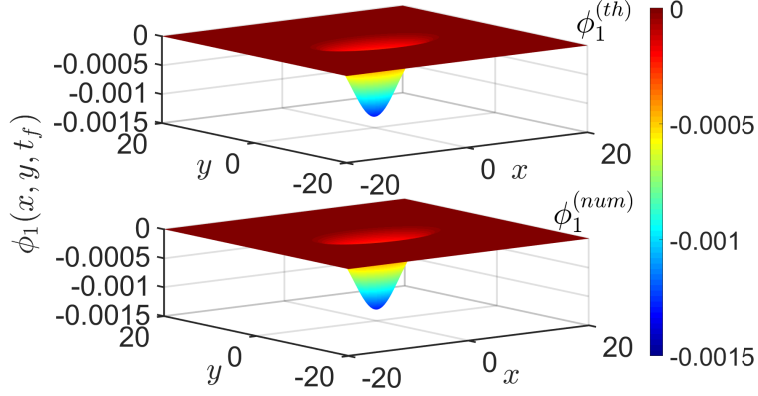


FIG. 7: (Color online) The collision-induced change in the shape of pulse 1  $\phi_1(x, y, t_f)$  at  $t_f = 1.6$  in a fast two-pulse collision with physical parameter values  $\epsilon_2 = 0.01$  and  $v_{d1} = 25$ . Top: the perturbation theory prediction of Eq. (60). Bottom: the result obtained by numerical solution of Eq. (57).

$\Delta\phi_1^{(r)}(y, t_f)$  obtained in the simulation with  $v_{d1} = 25$  [43]. A comparison with the perturbation theory prediction of Eqs. (61) and (60) is also shown. The agreement between the simulation result and the theoretical prediction is very good. The results in Figs. 7 and 8 and similar results that are obtained with other sets of the physical parameter values show that our perturbation method correctly captures the spatial distribution of the collision-induced change in the pulse shape.

We now turn to study the dependence of the fractional concentration reduction factor on the advection velocity. We characterize this dependence by measuring  $\Delta\phi_1^{(r)}(0, t_f)$  as a function of  $v_{d1}$ . Figure 9 shows the  $v_{d1}$  dependence of  $\Delta\phi_1^{(r)}(0, t_f)$  obtained in the simulations along with the theoretical prediction of Eqs. (61) and (60). The agreement between the simulations result and the perturbation theory prediction is excellent for all  $v_{d1}$  values,  $4 \leq |v_{d1}| \leq 60$ . In particular, the relative error in the approximation of  $\Delta\phi_1^{(r)}(0, t_f)$ , which is defined by  $|\Delta\phi_1^{(r)(num)}(0, t_f) - \Delta\phi_1^{(r)(th)}(0, t_f)| \times 100 / |\Delta\phi_1^{(r)(th)}(0, t_f)|$ , is smaller than 0.6% for  $10 \leq |v_{d1}| \leq 60$  and smaller than 1.4% for  $4 \leq |v_{d1}| < 10$ . We also studied the dependence of  $\Delta A_1^{(c)}$  on  $v_{d1}$ , and found very good agreement between the simulations result and the perturbation theory prediction (similar to what is shown in Figs. 2 and 4). Based on these results and on the results shown in Figs. 7 and 8 we conclude that the numerical simulations confirm the third major prediction of our generalized perturbation theory for

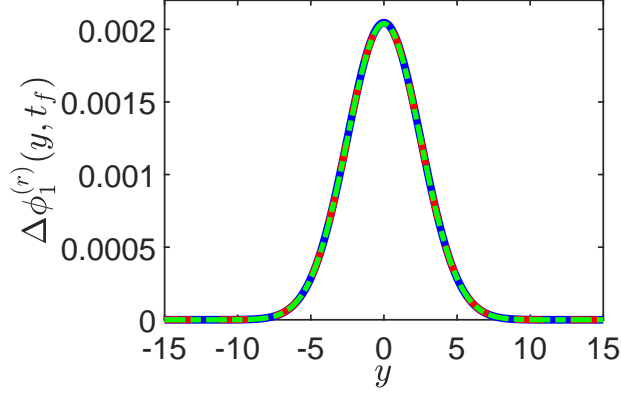


FIG. 8: (Color online) The fractional concentration reduction factor for pulse 1 at  $t = t_f$ ,  $\Delta\phi_1^{(r)}(y, t_f)$ , vs  $y$  in a two-pulse collision with parameter values  $\epsilon_2 = 0.01$  and  $v_{d1} = 25$ . The solid blue curve represents the perturbation theory prediction of Eqs. (61) and (60). The other two curves correspond to the results obtained by numerical solution of Eq. (57). The dashed red curve is obtained by averaging  $\Delta\phi_1^{(r)}(x, y, t_f)$  over the  $x$ -interval  $[-5, 5]$ . The dashed-dotted green curve is obtained by using the numerically computed value of  $\Delta\phi_1^{(r)}(0, y, t_f)$ .

the collision-induced change in the pulse shape in the direction transverse to the advection velocity vector.

#### IV. IMPORTANCE OF COLLISION-INDUCED EFFECTS DUE TO QUADRATIC LOSS

In the fast single-collision problem described by Eq. (1), the single-pulse evolution effects due to quadratic loss are of order  $\epsilon_2$  and higher, while the collisional effects due to quadratic loss are of order  $\epsilon_2/|v_{d1}|$  and higher. Thus, in this specific problem, the single-pulse evolution effects are stronger than the collision-induced effects. However, this does not reduce the importance of collision-induced effects due to quadratic loss in diffusion-advection systems, since there are many physical setups where the collisional effects can be comparable to or stronger than the single-pulse evolution effects. One can distinguish between two types of physical systems, for which the latter statement is valid. In the first type, which is described in subsection IIID, the rates of the reactions  $A + A \rightarrow A_2$  and  $B + B \rightarrow B_2$  are much smaller than the rate of the reaction  $A + B \rightarrow AB$ . As a result, in these systems, the collision-induced



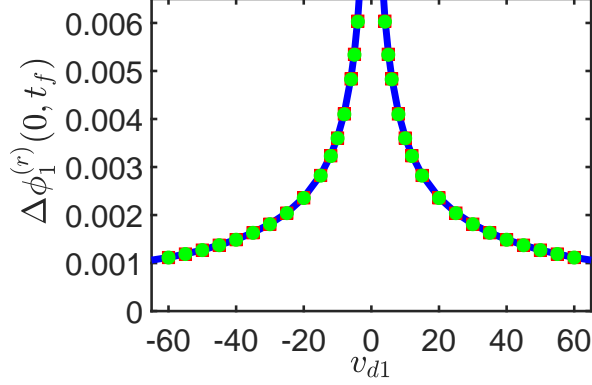


FIG. 9: (Color online) The fractional concentration reduction factor for pulse 1 at  $y = 0$  and  $t = t_f$ ,  $\Delta\phi_1^{(r)}(0, t_f)$ , vs advection velocity  $v_{d1}$  in a fast two-pulse collision with  $\epsilon_2 = 0.01$ . The solid blue curve corresponds to the perturbation theory prediction of Eqs. (61) and (60). The other two curves are obtained from the numerical solution of Eq. (57). The red squares represent the result obtained by averaging  $\Delta\phi_1^{(r)}(x, 0, t_f)$  over the  $x$ -interval  $[-5, 5]$ . The green circles represent the result obtained by using the numerically computed value of  $\Delta\phi_1^{(r)}(0, 0, t_f)$ .

effects due to quadratic loss are stronger than the corresponding single-pulse evolution effects already in the single-collision problem. In the second type of systems, the collisional effects due to quadratic loss are comparable to or stronger than the corresponding single-pulse evolution effects, even though the latter effects are stronger than the former in a single collision. This is the situation in physical systems containing a large number of pulses of different substances that are moving with different velocities, since the high collision rates in these systems can lead to dominance of the collisional effects compared with single-pulse evolution effects. An important example for this situation is provided by multisequence systems (including multisequence chemical communication links), where multiple pulse sequences move through the same medium with different velocities. In the current section, we briefly discuss the importance of collision-induced effects due to quadratic loss in comparison with single-pulse evolution effects due to quadratic loss in multisequence systems.

We start by considering two periodic pulse sequences of substances 1 and 2 (two gases), which are moving with different velocities through the same gaseous medium. We assume that the vector of relative velocity between the pulse sequences lies on the  $x$  axis, and denote the magnitude of this vector by  $|v_{d1}|$ . In addition, we denote the spatial separation (along

the  $x$  axis) between the centers of any two neighboring pulses in the two sequences by  $b$ . Then, the rate of collisions between a pulse from sequence 1 and pulses from sequence 2 is  $|v_{d1}|/b$ . As a result, the rate of change of the amplitude and shape of a pulse from sequence 1 due to collisions with sequence 2 pulses in the presence of weak quadratic loss is proportional to:

$$(|v_{d1}|/b) \times (-\epsilon_2/|v_{d1}|) = -\epsilon_2/b.$$

Therefore, the magnitude of the collisional effects is comparable to the magnitude of single-pulse evolution effects already in a two-sequence system. Furthermore, by a similar argument, in a system with  $N$  periodic pulse sequences of  $N$  different reacting substances, the rate of change of the amplitude and shape of a given pulse due to the cumulative effects of quadratic loss on the collisions is proportional to  $-(N-1)\epsilon_2/b$ . As a result, when  $N \gg 1$ , the collision-induced effects due to quadratic loss are dominant compared with the single-pulse evolution effects due to quadratic loss.

We emphasize that predictions about the importance of collision-induced effects in comparison with single-pulse evolution effects due to nonlinear dissipation in multisequence systems have been confirmed by extensive numerical simulations for propagation of multiple periodic sequences of optical solitons through an optical waveguide [37, 40, 44–46]. In this case, the dynamics is described by a system of perturbed nonlinear Schrödinger equations, where the dissipative perturbations are due to nonlinear loss and / or delayed Raman response [37, 40, 44–46]. The collision rate calculations for periodic sequences of pulses of the linear diffusion-advection system are essentially the same as the one used for multiple periodic soliton sequences in Refs. [37, 40, 44–46]. Therefore, the same conclusion is expected to hold for periodic sequences of the pulses considered in the current paper. That is, the collision-induced effects due to quadratic loss in the multisequence system can be comparable to or stronger than the single-pulse evolution effects due to quadratic loss, even though the latter effects are stronger than the former in a single collision.

## V. CONCLUSIONS

We investigated the dynamics of fast two-pulse collisions in linear diffusion-advection systems with weak quadratic loss in spatial dimension 2. The quadratic loss arises due to chemical reactions. We first introduced a two-dimensional perturbation method, which

generalizes the perturbation method used in Refs. [9, 10] for studying the one-dimensional collision problem in three important aspects. First, it extends the perturbative calculation from spatial dimension 1 to spatial dimension 2, and enables the extension of the calculation to a general spatial dimension. Second, it provides a calculation of the collision-induced dynamics of the pulse shape both in the collision interval and outside of the collision interval, whereas the calculation in Refs. [9, 10] was limited to the collision interval only. In this way, our generalized perturbation method enables for the first time an accurate comparison between perturbation theory predictions and numerical simulations results for the collision-induced change in the pulse shape. Third, it enables the discovery and analysis of several major collision-induced effects, which exist only in the high-dimensional problem. A key ingredient in the generalization of the perturbation method is the application of a rotation transformation, such that in the new coordinate system, the advection velocity vector lies on the  $x$ -axis. The application of this transformation enables one to overcome the main challenges in generalizing the perturbation method to spatial dimension higher than 1. More specifically, it enables one to preserve the true small parameters in the problem. Moreover, it simplifies the calculation, and in this manner, it enables the derivation of explicit expressions for the collision-induced changes in the pulse shape and amplitude.

We used the generalized perturbation method to obtain formulas for the collision-induced changes in the pulse shapes and amplitudes in spatial dimension 2. We showed that for a general initial condition, the collision induces a change in the pulse shape in the direction transverse to the advection velocity vector. We also considered the important case of a separable initial condition, and showed that in this case, the pulse shape in the longitudinal direction is not changed by the collision in the leading order of the perturbation theory. Furthermore, we found that for a separable initial condition, the longitudinal part in the expression for the collision-induced amplitude shift has a simple universal form. This finding is important, since it can be used in the design of scalable multisequence chemical communication links. Additionally, the transverse part in the expression for the amplitude shift was found to be nonuniversal, and proportional to the integral of the product of the pulse concentrations with respect to the transverse coordinate. We also showed that anisotropy in the initial condition leads to a complex dependence of the expression for the collision-induced amplitude shift on the orientation angle between the pulses. This complex dependence was attributed to the nonseparable nature of the initial condition in the anisotropic case.

We obtained very good agreement between our perturbation theory predictions and the results of extensive numerical simulations with the weakly perturbed diffusion-advection model for all the high-dimensional effects described in the preceding paragraph. Therefore, our work significantly enhanced and generalized the results of the previous studies in Refs. [9, 10] on fast two-pulse collisions in linear diffusion-advection systems with weak quadratic loss, which were limited to spatial dimension 1. Interestingly, we have recently found that similar high-dimensional effects exist in fast two-beam collisions in bulk linear optical media with weak cubic loss [31]. We emphasize that detailed analytic results on collisions between pulse solutions of linear or nonlinear evolution models in the presence of nonlinear dissipation in spatial dimension higher than 1 are scarce, and this is especially true for pulses that are not shape preserving. Therefore, the current study and our recent study in Ref. [31] also significantly extended the understanding of the general high-dimensional problem of fast two-pulse collisions in the presence of nonlinear dissipation.

### Appendix A: Invariance of $\Delta A_1^{(c)}$ under rotation transformations

In the current Appendix, we show that the change in the coordinate system, in which we rotate the  $x'$  and  $y'$  axes by an angle  $\Delta\theta$ , such that in the new coordinate system the advection velocity vector is on the  $x$  axis, does not change the value of  $\Delta A_1^{(c)}$ . That is, the value of  $\Delta A_1^{(c)}$  is invariant under rotation transformations in the  $xy$  plane. The change in the coordinate system and the associated invariance property are important for the following reasons. First, only the formulas obtained in the new coordinate system explicitly preserve the true small parameters in the problem. Second, the simpler form of the latter formulas enables the derivation of explicit expressions for  $\Delta A_1^{(c)}$ . In this manner, the application of the rotation transformation provides deeper insight into the collision dynamics in spatial dimension higher than 1.

Consider the fast collision problem in the  $(x', y', t)$  coordinate system, in which the advection velocity vector  $\mathbf{v}'_d = (v'_{d1}, v'_{d2})$  does not lie on the  $x'$  or  $y'$  axes. We assume that  $v'_d = |\mathbf{v}'_d| \gg 1$ . Therefore, the two small parameters in the problem are  $\epsilon_2$  and  $1/v'_d$ . The perturbed linear diffusion-advection model in the  $(x', y', t)$  coordinate system is

$$\begin{aligned}\partial_t u'_1 &= \partial_{x'}^2 u'_1 + \partial_{y'}^2 u'_1 - \epsilon_2 u_1'^2 - 2\epsilon_2 u'_2 u'_1, \\ \partial_t u'_2 &= \partial_{x'}^2 u'_2 + \partial_{y'}^2 u'_2 - v'_{d1} \partial_{x'} u'_2 - v'_{d2} \partial_{y'} u'_2 - \epsilon_2 u_2'^2 - 2\epsilon_2 u'_1 u'_2,\end{aligned}\tag{A1}$$

where  $u'_j(x', y', t)$  is the concentration of substance  $j$  in this coordinate system. The initial condition for the collision problem is:

$$u'_j(x', y', 0) = A_j(0)h'_j(x', y'). \quad (\text{A2})$$

We assume that the solution to the unperturbed diffusion equation

$$\partial_t u'_1 = \partial_{x'}^2 u'_1 + \partial_{y'}^2 u'_1 \quad (\text{A3})$$

does not contain any fast dependence on  $t$ . We also assume that the only fast dependence on  $t$  in the solution to the equation

$$\partial_t u'_2 = \partial_{x'}^2 u'_2 + \partial_{y'}^2 u'_2 - v'_{d1} \partial_{x'} u'_2 - v'_{d2} \partial_{y'} u'_2 \quad (\text{A4})$$

is contained in factors of the form  $x' - x'_{20} - v'_{d1}t$  and  $y' - y'_{20} - v'_{d2}t$ , where  $(x'_{20}, y'_{20})$  is the initial position of pulse 2 in the  $x'y'$  plane. When these assumptions are satisfied, we can use the perturbation method of subsection II B to show that the equation for  $\phi'_1$  in the collision interval in the leading order of the calculation is

$$\partial_t \phi'_1 = -2\epsilon_2 A_1(t) A_2(t) \tilde{u}'_{20} \tilde{u}'_{10}. \quad (\text{A5})$$

In addition, we can show by a similar calculation to the one carried out in subsection II B that  $\Delta\phi'_1(x', y', t_c)$  can be approximated by:

$$\begin{aligned} \Delta\phi'_1(x', y', t_c) &= -2\epsilon_2 A_1(t_c^-) A_2(t_c^-) \tilde{u}'_{10}(x', y', t_c) \\ &\times \int_{-\infty}^{\infty} dt' \bar{u}'_{20}(x' - x'_{20} - v'_{d1}t', y' - y'_{20} - v'_{d2}t', t_c). \end{aligned} \quad (\text{A6})$$

As a result, the collision-induced amplitude shift in the  $(x', y', t)$  coordinate system is

$$\begin{aligned} \Delta A'^{(c)}_1 &= -\frac{2\epsilon_2 A_1(t_c^-) A_2(t_c^-)}{C'_{d1}} \\ &\times \int_{-\infty}^{\infty} dx' \int_{-\infty}^{\infty} dy' \tilde{u}'_{10}(x', y', t_c) \int_{-\infty}^{\infty} dt' \bar{u}'_{20}(x' - x'_{20} - v'_{d1}t', y' - y'_{20} - v'_{d2}t', t_c), \end{aligned} \quad (\text{A7})$$

where

$$C'_{d1} = \int_{-\infty}^{\infty} dx' \int_{-\infty}^{\infty} dy' \tilde{u}'_{10}(x', y', 0). \quad (\text{A8})$$

Equation (A7) does not explicitly preserve the true small parameters in the problem  $\epsilon_2$  and  $1/v'_d$ , since it contains *two* parameters  $v'_{d1}$  and  $v'_{d2}$  that are associated with  $v'_d$ . Moreover, the

integration variable  $t'$  appears in the expression for  $\bar{u}'_{20}$  in the inner integral twice, and as a result, derivation of explicit formulas for the amplitude shift from Eq. (A7) is challenging.

We now apply a rotation transformation from the  $(x', y', t)$  coordinate system to the  $(x, y, t)$  coordinate system, in which the advection velocity vector is on the  $x$  axis. The rotation angle is  $\Delta\theta = \arctan(v'_{d2}/v'_{d1})$ , and the equations that define the transformation are:

$$\begin{aligned}x' &= x \cos \Delta\theta - y \sin \Delta\theta, \\y' &= x \sin \Delta\theta + y \cos \Delta\theta,\end{aligned}\tag{A9}$$

and

$$u'_j(x', y', t) = u_j(x, y, t).\tag{A10}$$

One can show that the perturbed linear diffusion-advection model in the  $(x, y, t)$  system is Eq. (1), where  $|v_{d1}| = v'_d$ . The initial condition for the two-pulse collision problem is given by Eq. (2), where  $h_j(x, y) = h'_j(x', y')$ . Since the only large parameter in Eq. (1) is  $|v_{d1}|$ , the transformation in Eqs. (A9) and (A10) does not change the properties of the fast dependence on  $t$  of the solutions to the unperturbed diffusion equations (A3) and (A4). That is, the solution to the unperturbed equation

$$\partial_t u_1 = \partial_x^2 u_1 + \partial_y^2 u_1\tag{A11}$$

does not contain any fast dependence on  $t$ , and the only fast dependence on  $t$  in the solution to the equation

$$\partial_t u_2 = \partial_x^2 u_2 + \partial_y^2 u_2 - v_{d1} \partial_x u_2\tag{A12}$$

is contained in factors of the form  $x - x_{20} - v_{d1}t$ . It follows that we can calculate the collision-induced amplitude shift  $\Delta A_1^{(c)}$  in the  $(x, y, t)$  system by the perturbation method of subsection II B. Moreover, the result of this calculation is that  $\Delta A_1^{(c)}$  is given by Eqs. (17) and (16).

We now show that the amplitude shift value  $\Delta A_1'^{(c)}$  in Eq. (A7) is equal to the value of  $\Delta A_1^{(c)}$  in Eq. (17). We first note that the Jacobian of the transformation (A9) is equal to 1. Using this together with Eqs. (16), (A8), and (A10), we find  $C'_{d1} = C_{d1}$ . Second, from Eq. (A10) it follows that  $\tilde{u}'_{j0}(x', y', t_c) = \tilde{u}_{j0}(x, y, t_c)$ . Third, since the transformation in Eqs.

(A9)-(A10) does not change the properties of the fast dependence on  $t$  of the solutions to the unperturbed diffusion equations, and since  $v_{d2} = 0$ , we obtain [47]:

$$\bar{u}'_{20}(x' - x'_{20} - v'_{d1}t, y' - y'_{20} - v'_{d2}t, t_c) = \bar{u}_{20}(x - x_{20} - v_{d1}t, y, t_c). \quad (\text{A13})$$

Substituting all these relations into Eq. (A7), we obtain:

$$\Delta A_1'^{(c)} = -\frac{2\epsilon_2 A_1(t_c^-) A_2(t_c^-)}{C_{d1}|v_{d1}|} \int_{-\infty}^{\infty} dx \int_{-\infty}^{\infty} dy \tilde{u}_{10}(x, y, t_c) \int_{-\infty}^{\infty} d\tilde{x} \bar{u}_{20}(\tilde{x}, y, t_c) = \Delta A_1^{(c)}. \quad (\text{A14})$$

Therefore, the value of  $\Delta A_1^{(c)}$  is invariant under rotation transformations in the  $xy$  plane.

## Appendix B: Amplitude dynamics in the perturbed single-pulse evolution problem

In this Appendix, we obtain the equation for the dynamics of pulse amplitudes in the perturbed single-pulse evolution problem. This equation is used in the calculation of the amplitude values in the approximate expressions (8) for the  $u_{j0}$ , and also in the calculation of  $A_j(t_c^-)$  in the equations for  $\Delta\phi_1(x, y, t_c)$  and  $\Delta A_1^{(c)}$  in sections II and III.

We consider the dynamic evolution of a single pulse in the presence of diffusion, advection, and weak quadratic loss. The dynamics is described by Eqs. (5) and (6) for pulses 1 and 2, respectively. Using mass balance calculations for these equations, we find

$$\partial_t \int_{-\infty}^{\infty} dx \int_{-\infty}^{\infty} dy u_{j0}(x, y, t) = -\epsilon_2 \int_{-\infty}^{\infty} dx \int_{-\infty}^{\infty} dy u_{j0}^2(x, y, t). \quad (\text{B1})$$

We substitute the approximate expressions (8) for the  $u_{j0}$  into Eq. (B1), and obtain the following equation for the dynamics of the  $A_j$ :

$$C_{dj} \frac{dA_j}{dt} = -\epsilon_2 P_{2j}(t) A_j^2. \quad (\text{B2})$$

In Eq. (B2),  $P_{2j}(t) = \int_{-\infty}^{\infty} dx \int_{-\infty}^{\infty} dy \tilde{u}_{j0}^2(x, y, t)$ ,  $C_{d1}$  is given by Eq. (16), and  $C_{d2}$  is given by a similar equation, in which  $\tilde{u}_{10}(x, y, 0)$  is replaced by  $\tilde{u}_{20}(x, y, 0)$ . The solution of Eq. (B2) on the time interval  $[0, t]$  is

$$A_j(t) = \frac{A_j(0)}{1 + \epsilon_2 \tilde{P}_{2j}(0, t) A_j(0) / C_{dj}}, \quad (\text{B3})$$

where  $\tilde{P}_{2j}(0, t) = \int_0^t dt' P_{2j}(t')$ . The effects of linear loss on the dynamics of pulse amplitudes can be included in the perturbative calculation in the same manner as was done in Refs. [9, 10] for the one-dimensional problem. Furthermore, similar to the one-dimensional problem, it can be shown that these effects do not alter the form of the expressions for the collision-induced changes in pulse amplitudes and shapes.

### Appendix C: The solution of the unperturbed diffusion equation with a Gaussian initial condition

We present here a very brief summary of the formulas for the solution of the unperturbed linear diffusion equation with a Gaussian initial condition, since this solution is used extensively in section III, as an example. We consider the unperturbed linear diffusion equation

$$\partial_t u = \partial_x^2 u + \partial_y^2 u \quad (\text{C1})$$

with the separable Gaussian initial condition

$$u(x, y, 0) = A \exp \left[ -\frac{(x - x_0)^2}{2W_0^{(x)2}} - \frac{(y - y_0)^2}{2W_0^{(y)2}} \right]. \quad (\text{C2})$$

The solution of Eq. (C1) with the initial condition (C2) can be written as:

$$u(x, y, t) = A g^{(x)}(\tilde{x}, t) g^{(y)}(\tilde{y}, t), \quad (\text{C3})$$

where  $\tilde{x} = x - x_0$ ,  $\tilde{y} = y - y_0$ ,

$$g^{(x)}(\tilde{x}, t) = \frac{W_0^{(x)}}{(W_0^{(x)2} + 2t)^{1/2}} \exp \left[ -\frac{\tilde{x}^2}{2W_0^{(x)2} + 4t} \right], \quad (\text{C4})$$

and

$$g^{(y)}(\tilde{y}, t) = \frac{W_0^{(y)}}{(W_0^{(y)2} + 2t)^{1/2}} \exp \left[ -\frac{\tilde{y}^2}{2W_0^{(y)2} + 4t} \right]. \quad (\text{C5})$$

In addition, the solution of Eq. (C1) with the term  $-v_{d1} \partial_x u$  on its right hand side and with the initial condition (C2) is given by Eqs. (C3)-(C5) with  $\tilde{x} = x - x_0 - v_{d1}t$ , and  $\tilde{y} = y - y_0$ .

### Appendix D: Derivation of Eq. (59)

We present the derivation of Eq. (59) for the inverse Fourier transform of  $\hat{g}_{12}^{(y)}(k_2, t_c) \exp[-k_2^2(t - t_c)]$ . This equation is used in subsection IIID in the calculation of  $\phi_1(x, y, t)$  in the post-collision interval, in the case where the initial condition for the collision problem is given by the Gaussian pulses of Eq. (39).

Using Eqs. (35) and (C5), we obtain:

$$g_{12}^{(y)}(y, t_c) = \frac{W_{10}^{(y)} W_{20}^{(y)} \exp[-\tilde{a}_2^2(t_c) y^2]}{(W_{10}^{(y)2} + 2t_c)^{1/2} (W_{20}^{(y)2} + 2t_c)^{1/2}}, \quad (\text{D1})$$



where

$$\tilde{a}_2^2(t_c) = \frac{W_{10}^{(y)2} + W_{20}^{(y)2} + 4t_c}{2(W_{10}^{(y)2} + 2t_c)(W_{20}^{(y)2} + 2t_c)}. \quad (\text{D2})$$

The Fourier transform of  $g_{12}^{(y)}(y, t_c)$  is:

$$\hat{g}_{12}^{(y)}(k_2, t_c) = \frac{W_{10}^{(y)} W_{20}^{(y)}}{(W_{10}^{(y)2} + W_{20}^{(y)2} + 4t_c)^{1/2}} \exp \left[ -\frac{k_2^2}{4\tilde{a}_2^2(t_c)} \right]. \quad (\text{D3})$$

As a result, we obtain the following expression for the inverse Fourier transform of  $\hat{g}_{12}^{(y)}(k_2, t_c) \exp[-k_2^2(t - t_c)]$ :

$$\begin{aligned} \mathcal{F}^{-1} \left( \hat{g}_{12}^{(y)}(k_2, t_c) \exp[-k_2^2(t - t_c)] \right) &= \frac{W_{10}^{(y)} W_{20}^{(y)}}{(W_{10}^{(y)2} + 2t_c)^{1/2} (W_{20}^{(y)2} + 2t_c)^{1/2} [1 + 4\tilde{a}_2^2(t_c)(t - t_c)]^{1/2}} \\ &\times \exp \left[ -\frac{\tilde{a}_2^2(t_c) y^2}{1 + 4\tilde{a}_2^2(t_c)(t - t_c)} \right]. \end{aligned} \quad (\text{D4})$$

Equation (D4) is Eq. (59) of subsection III D.

- 
- [1] N.G. Van Kampen, *Stochastic Processes in Physics and Chemistry* (Elsevier, Amsterdam, 2007).
  - [2] G.B. Whitham, *Linear and Nonlinear Waves* (Wiley, New York, 1999).
  - [3] E. Merzbacher, *Quantum Mechanics* (Wiley, New York, 1998).
  - [4] A. Ishimaru, *Electromagnetic Wave Propagation, Radiation, and Scattering* (Wiley, Hoboken, NJ, 2017).
  - [5] A.E. Siegman, *Lasers* (University Science Books, Mill Valley, CA, 1986).
  - [6] H. Kogelnik and T. Li, *Appl. Opt.* **5**, 1550 (1966).
  - [7] Q. Lin, O.J. Painter, and G.P. Agrawal, *Opt. Express* **15**, 16604 (2007).
  - [8] P. Érdi and J. Tóth, *Mathematical Models of Chemical Reactions: Theory and Applications of Deterministic and Stochastic Models* (Manchester University Press, Manchester, UK, 1989).
  - [9] A. Peleg, Q.M. Nguyen, and T.T. Huynh, *Eur. Phys. J. D* **71**, 315 (2017).
  - [10] Q.M. Nguyen, T.T. Huynh, and A. Peleg, *Indian J. Phys.* **96**, 453 (2022).
  - [11] Fast two-pulse collisions are collisions, in which the time interval during which the two pulses overlap (the collision duration) is much smaller than all the other time scales in the problem. In particular, in the case of a fast two-pulse collision in weakly perturbed linear diffusion-advection systems, the collision duration is much smaller than the diffusion time [9, 10].

- [12] Q.M. Nguyen, Int. J. Nonlinear Sci. Numer. Simulat. **23**, 335 (2022).
- [13] F. Forghieri, R.W. Tkach, and A.R. Chraplyvy, in *Optical Fiber Telecommunications III A*, I.P. Kaminow and T.L. Koch, eds., (Academic, San Diego, CA, 1997), Chapter 8.
- [14] G.P. Agrawal, P.L. Baldeck, and R.R. Alfano, Phys. Rev. A **39**, 3406 (1989).
- [15] R. Hui, K.R. Demarest, and C.T. Allen, J. of Lightwave Technol. **17**, 1018 (1999).
- [16] G.P. Agrawal, *Nonlinear Fiber Optics* (Academic, San Diego, CA, 2019).
- [17] A. Peleg, M. Chertkov, and I. Gabitov, Phys. Rev. E **68**, 026605 (2003).
- [18] G.P. Agrawal, *Fiber-Optic Communication Systems* (Wiley, New York, NY, 1997).
- [19] A.H. Gnauck, R.W. Tkach, A.R. Chraplyvy, and T. Li, J. Lightwave Technol. **26**, 1032 (2008).
- [20] L.F. Mollenauer, A. Grant, X. Liu, X. Wei, C. Xie, and I. Kang, Opt. Lett. **28**, 2043 (2003).
- [21] M. Nakazawa, IEEE J. Sel. Top. Quant. Electron. **6**, 1332 (2000).
- [22] M.K. McClintock, Horm. Behav. **10**, 264 (1978).
- [23] M.A. Farag, H. Zhang, and C.-M. Ryu, J. Chem. Ecol. **39**, 1007 (2013).
- [24] W.C. Agosta, *Chemical Communication: The Language of Pheromones* (W.H. Freeman, New York, NY 1992).
- [25] T.D. Wyatt, *Pheromones and Animal Behaviour: Communication by Smell and Taste* (Cambridge University Press, Cambridge, 2003).
- [26] B.D. Unluturk and I.F. Akyildiz, IEEE Trans. Nanobiosci. **16**, 11 (2017).
- [27] A.W. Czarnik, Acc. Chem. Res. **27**, 302 (1994).
- [28] C. Brönmark and L.-A. Hansson, Oikos **88**, 103 (2000).
- [29] D.T. McGuinness, S. Giannoukos, A. Marshall, and S. Taylor, IEEE Access **6**, 46706 (2018).
- [30] D.T. McGuinness, S. Giannoukos, S. Taylor, and A. Marshall, IEEE Trans. Mol. Biol. Multi-Scale Commun. **6**, 93 (2020).
- [31] A. Peleg, T.T. Huynh, and Q.M. Nguyen, J. Eng. Math. **132**, 23 (2022).
- [32] The dimensionless coordinates  $x$  and  $y$  in Eq. (1) are  $x = X/x_0$  and  $y = Y/x_0$ , where  $X$  and  $Y$  are the dimensional coordinates, and  $x_0$  is the width of a reference pulse in the  $x$  direction. The dimensionless time is  $t = \tau/\tau_D$ , where  $\tau$  is time,  $\tau_D = x_0^2/D$ , and  $D$  is the dimensional diffusion coefficient.  $u_j = U_j/\rho_0$ , where  $U_j$  is the concentration of substance  $j$  and  $\rho_0$  is the peak concentration.  $v_{d1} = x_0 V_{d1}/D$ , where  $V_{d1}$  is the dimensional advection velocity (the dimensional velocity difference between the two pulses).  $\epsilon_2 = \rho_0 x_0^2 \tilde{\epsilon}_2/D$ , where  $\tilde{\epsilon}_2$  is the dimensional quadratic loss coefficient.

- [33] A.B. Koudriavtsev, R.F. Jameson, and W. Linert, *The Law of Mass Action* (Springer, Berlin, 2001).
- [34] T. Turányi and A.S. Tomlin, *Analysis of Kinetic Reaction Mechanisms* (Springer, Berlin, 2014).
- [35] E.O. Voit, H.A. Martens, and S.W. Omholt, PLoS Comput. Biol. **11**, e1004012 (2015).
- [36] D.R. Lide, ed., *CRC Handbook of Chemistry and Physics* (CRC Press, Boca Raton, FL, 2004), p. 6-179.
- [37] A. Peleg, Q.M. Nguyen, and Y. Chung, Phys. Rev. A **82**, 053830 (2010).
- [38] A form similar to Eq. (32) was obtained in Ref. [31] for fast collisions between beams of the linear propagation equation.
- [39] W.H. Hundsdorfer and J.G. Verwer, *Numerical Solution of Time Dependent Advection-Diffusion-Reaction Equations* (Springer, New York, 2003).
- [40] A. Peleg and Y. Chung, Phys. Rev. A **85**, 063828 (2012).
- [41] The values of  $t_i$  are determined by:  $t_i = t_c + r(t_f - t_c)$ , where  $r = 1/5$ , as an example. Therefore,  $t_i$  is an intermediate time that is larger than  $t_c$ , at which the collision is not yet completed.
- [42] In subsection IIID, the coefficient  $\tilde{a}_1$  depends on  $A_1(0)$  and  $A_2(0)$  instead of on  $A_1(t_c^-)$  and  $A_2(t_c^-)$ . Therefore, we replace the notation  $\tilde{a}_1(t_c^-)$  by  $\tilde{a}_1$  in this subsection.
- [43] Since the fractional concentration reduction factor obtained in the simulation  $\Delta\phi_1^{(r)(num)}(x, y, t)$  shows weak dependence on  $x$ , we use two different methods to obtain  $\Delta\phi_1^{(r)}(y, t)$  from the simulation result. In the first method, we calculate  $\Delta\phi_1^{(r)}(y, t)$  by averaging  $\Delta\phi_1^{(r)(num)}(x, y, t)$  over the  $x$ -interval  $[-5, 5]$ , and in the second method, we use the value of  $\Delta\phi_1^{(r)(num)}(0, y, t)$ .
- [44] A. Peleg, Q.M. Nguyen, and T.P. Tran, Opt. Commun. **380**, 41 (2016).
- [45] A. Peleg, Q.M. Nguyen, and T.T. Huynh, Eur. Phys. J. D **71**, 30 (2017).
- [46] A. Peleg and D. Chakraborty, Commun. Nonlinear Sci. Numer. Simulat. **63**, 145 (2018).
- [47] Note that  $\bar{u}_{20}$  depends on  $y_{20}$ . However, for brevity of notation, we did not write this dependence explicitly in Eq. (A13) and throughout the paper.